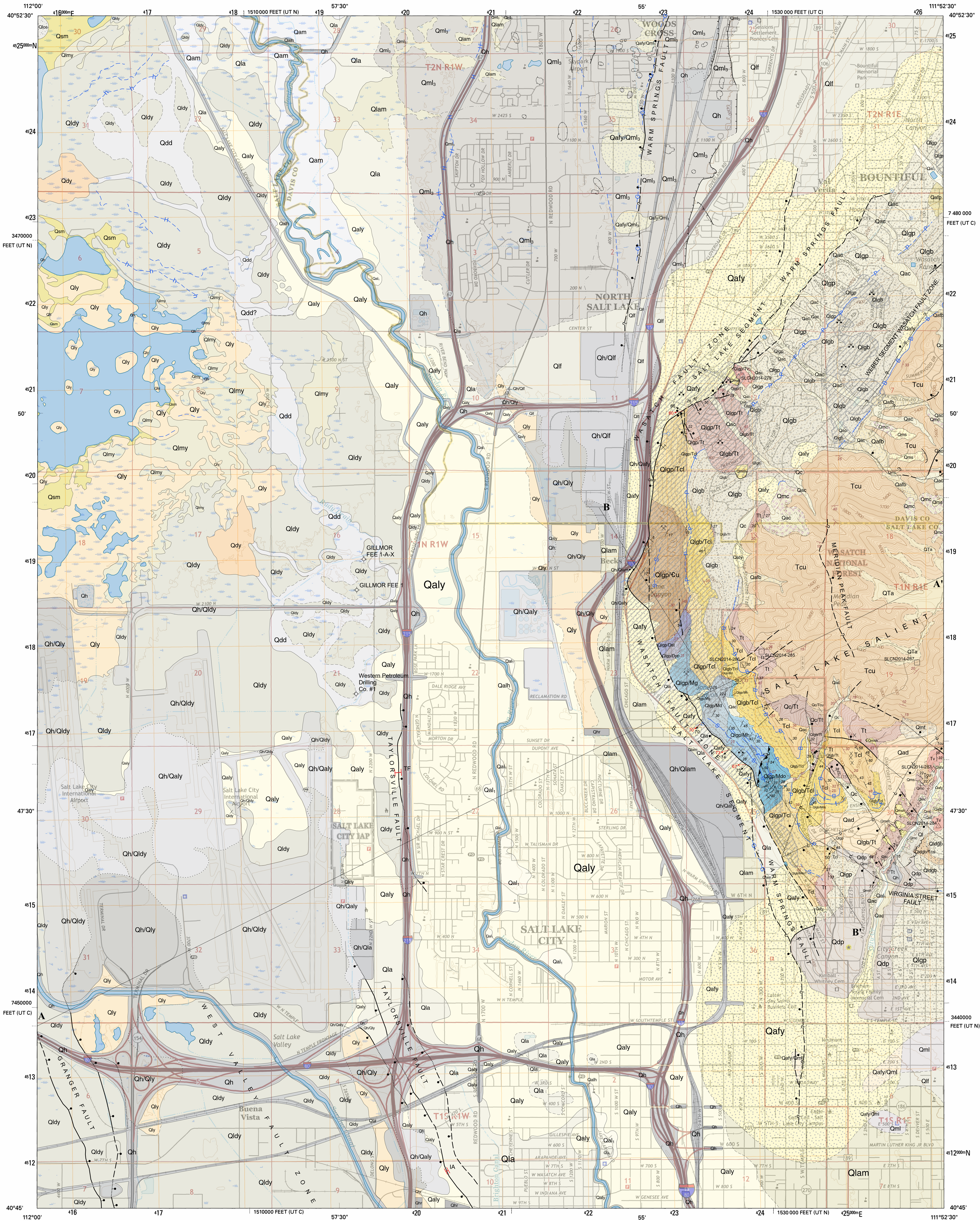

SCALE 1:24,000

1 0.5 0 1 MILE

1000 0 1000 2000 3000 4000 5000 6000 7000 FEET

1 0.5 0 1 KILOMETER

CONTOUR INTERVAL 20 FEET

This open-file release makes information available to the public that has undergone only minimal peer review and may not conform to Utah Geological Survey technical, editorial, or policy standards. The map may be incomplete, and inconsistencies, errors, and omissions have not been resolved. The Utah Department of Natural Resources, Utah Geological Survey, makes no warranty, expressed or implied, regarding the suitability of this product for a particular use, and does not guarantee accuracy or completeness of the data. The Utah Department of Natural Resources, Utah Geological Survey, shall not be liable under any circumstances for any direct, indirect, special, incidental, or consequential damages with respect to claims by users of this product. For use at 1:24,000 scale.

This geologic map was funded by the Utah Geological Survey and the U.S. Geological Survey, National Cooperative Geologic Mapping Program, through USGS STATEMAP award number G13AC00169 (2013–2014). The views and conclusions contained in this document are those of the authors and should not be interpreted as necessarily representing the official policies, either expressed or implied, of the U.S. Government.

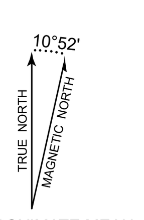

APPROXIMATE MEAN DECLINATION, 2024

INTERIM GEOLOGIC MAP OF THE SALT LAKE CITY NORTH QUADRANGLE, SALT LAKE AND DAVIS COUNTIES, UTAH

by

Adam P. McKean and Zachary W. Anderson

2024

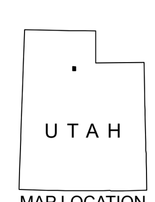

MAP LOCATION

Base from USGS US Topo Salt Lake City North 7.5' Quadrangle (2017). Projection and datum for base map and GIS data are UTM Zone 12 N NAD83.

Project Manager: Donald L. Clark
Aerial photo and field mapping of geology:
Adam P. McKean, 2013–2014, 2018–2021, 2023
Zachary W. Anderson, 2016–2018, 2021–2023
GIS and Cartography: Adam P. McKean and Austin J. Jensen
GIS and Cartographic Review: Josh Dustin and Subigya Shah

Utah Geological Survey
1594 West North Temple, Suite 3110
Salt Lake City, UT 84116
(801) 537-3300
geology.utah.gov

https://doi.org/10.34191/OFR-768DM

1	2	3
4		5
6	7	8

1. Saltair NE
2. Farmington
3. Bountiful Peak
4. Baileys Lake
5. Fort Douglas
6. Magna
7. Salt Lake City South
8. Sugar House

ADJOINING 7.5' QUADRANGLE NAMES

MAP UNITS
(see booklet for complete unit descriptions)

- Qal_1 Active stream and floodplain deposits
- Qaly Young floodplain and stream deposits, undivided
- Qatp Stream terrace deposits, related to Provo shoreline and regressive phase of Lake Bonneville
- Qafy Younger alluvial-fan deposits, undivided
- Qafp Alluvial-fan deposits, related to Provo shoreline and regressive phase of Lake Bonneville
- Qafb Alluvial-fan deposits, related to Bonneville shoreline and transgressive phase of Lake Bonneville
- Qc Colluvial deposits
- Qh Fill and disturbed land
- Qhr Remediated land
- Qdy Young deltaic deposits related to Great Salt Lake
- Qdd Deltaic distributary channel deposits related to Great Salt Lake
- Qlos Lacustrine oolitic sand deposits related to Great Salt Lake
- Qldy Young lacustrine and deltaic deposits related to Great Salt Lake, Gilbert-episode lake, and Lake Bonneville
- Qlmy Young lacustrine mud deposits related to Great Salt Lake, Gilbert-episode lake, and Lake Bonneville
- Qly Young lacustrine deposits related to Great Salt Lake, Gilbert-episode lake, and Lake Bonneville
- Qlf Lacustrine fine-grained deposits related to Great Salt Lake, Gilbert-episode lake, and Lake Bonneville
- Ql Lake Bonneville and pre-Bonneville deposits, undivided
- Qdp Deltaic deposits related to the Provo shoreline and regressive phase of Lake Bonneville
- Qlgp Lacustrine gravel and sand related to the Provo shoreline and regressive phase of Lake Bonneville
- Qldgb Lacustrine and deltaic gravel and sand related to the Bonneville shoreline and transgressive phase of Lake Bonneville
- Qlgb Lacustrine gravel and sand related to the Bonneville shoreline and transgressive phase of Lake Bonneville
- Qml Lateral spread deposits
- Qml_3 North Salt Lake lateral spread deposit
- Qmsh Historical landslide deposits
- Qms Landslide deposits
- Qmt Talus deposits
- Qsm Spring and marsh deposits
- Qalh Historical alluvial deposits and artificial levees, undivided
- Qac Alluvial and colluvial deposits, undivided
- Qad Alluvial-fan and Lake Bonneville deltaic deposits, undivided
- Qam Alluvial and marsh deposits
- Qla Lacustrine and alluvial deposits, undivided
- Qlam Lacustrine, alluvial, and marsh deposits, undivided
- Qmc Landslide and colluvium deposits, undivided
- $Qafy/Qml_3$ Younger alluvial-fan deposits, undivided over North Salt Lake lateral spread deposit
- Qafy/Qml Younger alluvial-fan deposits, undivided over lateral spread deposits
- Qc/Tcu Colluvial deposits over upper conglomerate
- Qc/Tt Colluvial deposits over tuffaceous strata
- Qh/Qaly Fill and disturbed land over young stream deposits, undivided
- Qh/Qafy Fill and disturbed land over younger alluvial-fan deposits
- Qh/Qly Fill and disturbed land over young lacustrine deposits of Great Salt Lake, Gilbert-episode lake, and Lake Bonneville
- Qh/Qlf Fill and disturbed land over lacustrine fine-grained undivided deposits of Lake Bonneville, Gilbert episode lake, and Great Salt Lake
- Qh/Qldy Fill and disturbed land over young lacustrine and deltaic deposits of Great Salt Lake, Gilbert-episode lake, and Lake Bonneville
- Qh/Qla Fill and disturbed land over lacustrine and alluvial deposits, undivided
- Qh/Qlam Fill and disturbed land over lacustrine, alluvial, and marsh deposits, undivided
- Qlgp/Tv Lacustrine gravel and sand related to the Provo shoreline and regressive phase of Lake Bonneville over volcaniclastic conglomerate
- Qlgp/Tt Lacustrine gravel and sand related to the Provo shoreline and regressive phase of Lake Bonneville over tuffaceous strata
- Qlgp/Tcl Lacustrine gravel and sand related to the Provo shoreline and regressive phase of Lake Bonneville over lower conglomerate
- Qlgp/Mdo Lacustrine gravel and sand related to the Provo shoreline and regressive phase of Lake Bonneville over Doughnut Formation
- Qlgp/Mh Lacustrine gravel and sand related to the Provo shoreline and regressive phase of Lake Bonneville over Humbug Formation
- Qlgp/Md Lacustrine gravel and sand related to the Provo shoreline and regressive phase of Lake Bonneville over Deseret Limestone
- Qlgp/Mg Lacustrine gravel and sand related to the Provo shoreline and regressive phase of Lake Bonneville over Gardison Limestone
- Qlgp/Dpp Lacustrine gravel and sand related to the Provo shoreline and regressive phase of Lake Bonneville over Pinyon Peak Limestone
- Qlgp/Dst Lacustrine gravel and sand related to the Provo shoreline and regressive phase of Lake Bonneville over Stansbury Formation
- Qlgp/Ꞓu Lacustrine gravel and sand related to the Provo shoreline and regressive phase of Lake Bonneville over Cambrian strata, undivided
- Qldgb/Tcu Deltaic deposits related to the Bonneville shoreline and transgressive phase of Lake Bonneville over upper conglomerate
- Qlgb/Tt Lacustrine gravel and sand related to the Bonneville shoreline and transgressive phase of Lake Bonneville over tuffaceous strata
- Qlgb/Tcl Lacustrine gravel and sand related to the Bonneville shoreline and transgressive phase of Lake Bonneville over lower conglomerate
- Qlgb/Mdo Lacustrine gravel and sand related to the Bonneville shoreline and transgressive phase of Lake Bonneville over Doughnut Formation
- Qlgb/Mh Lacustrine gravel and sand related to the Bonneville shoreline and transgressive phase of Lake Bonneville over Humbug Formation
- Qlgb/Md Lacustrine gravel and sand related to the Bonneville shoreline and transgressive phase of Lake Bonneville over Deseret Limestone
- Qlgb/Ꞓu Lacustrine gravel and sand related to the Bonneville shoreline and transgressive phase of Lake Bonneville over Cambrian strata, undivided
- QTa Old alluvial deposits
- Tcu Upper conglomerate
- Tv Volcaniclastic conglomerate
- Tt Tuffaceous strata
- Tcl Lower conglomerate
- Mdo Doughnut Formation (see cross sections and stacked units)
- Mh Humbug Formation (see cross sections and stacked units)
- Md Deseret Limestone (see cross sections and stacked units)
- Mg Gardison Limestone (see cross sections and stacked units)
- Dpp Pinyon Peak Limestone (see cross sections and stacked units)
- Dst Stansbury Formation (see cross sections and stacked units)
- Ꞓu Cambrian strata, undivided (see cross sections and stacked units)
- Ꞓo Ophir Formation (see cross sections)
- Ꞓt Tintic Quartzite (see cross sections)

LITHOLOGIC COLUMN

AGE			GEOLOGIC UNIT		MAP UNIT SYMBOL	THICKNESS Feet (Meters)		LITHOLOGY
QUAT.		PLEIS.	Old alluvial deposits*		QTa	20–60 (6–18)		Unconformity
TERTIARY	NEOGENE	PLIO.						
TERTIARY	NEOGENE	MIO. / OLIGO.	Upper conglomerate		Tcu	500–1600 (150–500)		Unconformity
TERTIARY	PALEOGENE	EOCENE	Volcaniclastic conglomerate		Tv	0–500 (0–150)		35 to 38 Ma K-Ar (Van Horn, 1981); 39 Ma $^{40}Ar/^{39}Ar$; Minor Unconformity
TERTIARY	PALEOGENE	EOCENE	Tuffaceous strata		Tt	30–1200 (10–360)		44 Ma Zircon U-Pb; 45 Ma K-Ar (Van Horn, 1981); Unconformity
TERTIARY	PALEOGENE	PALEO.	Lower conglomerate		Tcl	600–1150 (180–350)		48 Ma Zircon U-Pb; Major Unconformity
MISSISSIPPIAN	LATE		Doughnut Formation		Mdo	800+ (240+)		
MISSISSIPPIAN	LATE		Humbug Formation		Mh	1000–1400 (300–425)		
MISSISSIPPIAN	LATE		Deseret Limestone		Md	500–800 (150–250)		Delle Phosphatic Member?
MISSISSIPPIAN	EARLY		Gardison Limestone		Mg	850–950 (260–290)		Unconformity
DEVONIAN	LATE		Pinyon Peak Limestone		Dpp	130–200 (40–60)		
DEVONIAN	LATE		Stansbury Formation		Dst	270–300 (80–90)		Major Unconformity (Stansbury uplift); Major Unconformity (Tooele arch)
CAMBRIAN	LATE		Camrbian bedrock, undivided	St. Charles Formation	Ꞓu	1200+ (360+)	440–520 (130–160)	
CAMBRIAN	LATE			Nounan Formation			550–590 (160–180)	
CAMBRIAN	MIDDLE			Bloomington Formation			200–350 (60–110)	
CAMBRIAN	MIDDLE			Maxfield Limestone			610–830 (186–253)	Base not exposed in quadrangle
CAMBRIAN	MIDDLE		Ophir Formation		Ꞓo	300–380 (90–115)		Subsurface only
CAMBRIAN	E.?		Tintic Quartzite		Ꞓt	1500–1970 (450–600)		Not exposed in quadrangle

See Subsurface Units section for discussion of concealed Precambrian metamorphic bedrock
*Could be semiconsolidated to unconsolidated
Not to scale

CORRELATION OF GEOLOGIC UNITS

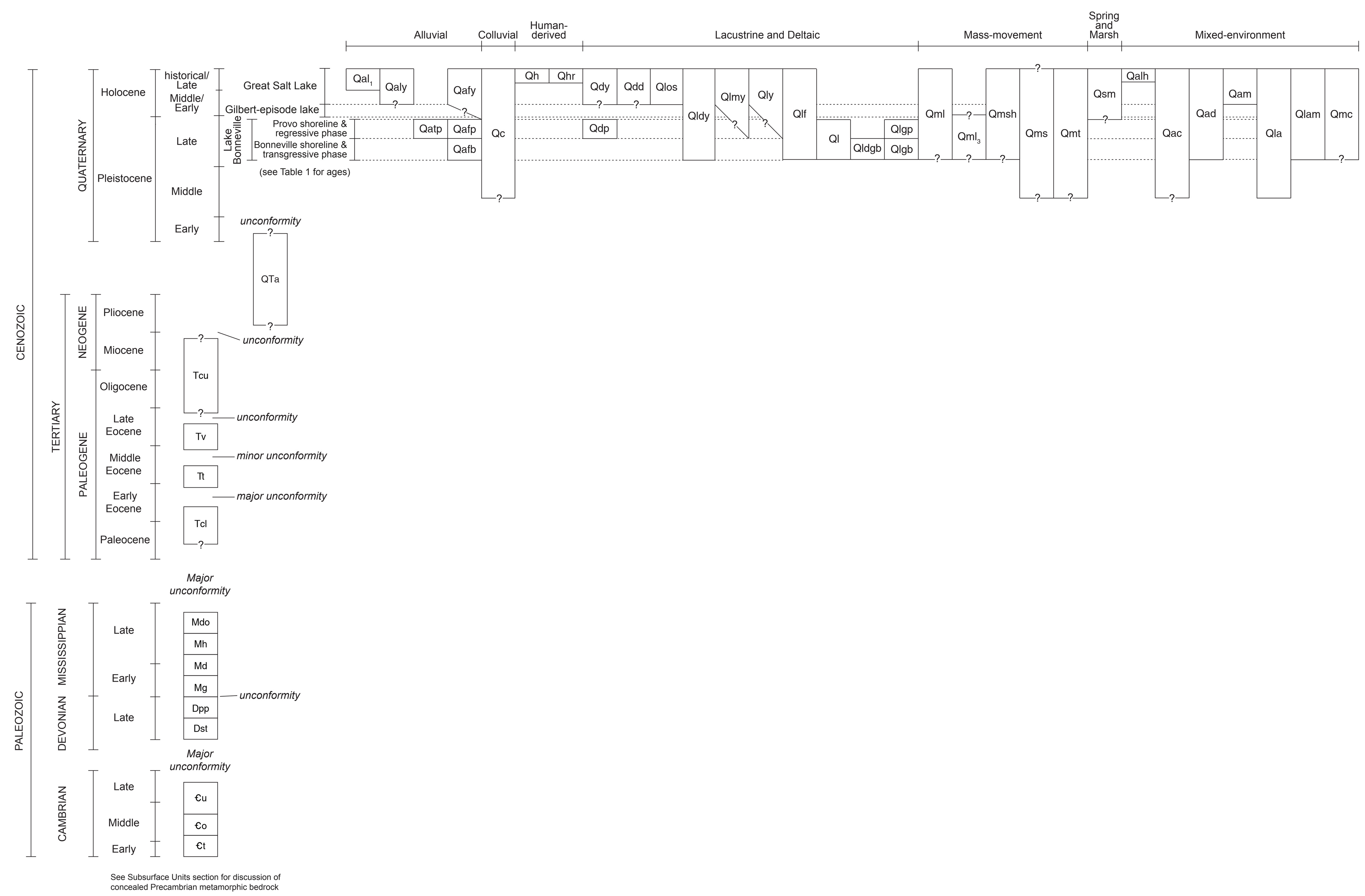

GEOLOGIC MAP SYMBOLS

- Contact – Dashed where approximately located; dotted where concealed
- Contact, internal
- 74 70 Normal fault – Dashed where approximately located, dotted where concealed; bar and ball on downthrown side; queried where existence is uncertain; black arrows and text show fault plane dip direction and dip; red arrows show averaged fault trend and plunge of fault slickenlines; arrows on cross section indicate direction of relative movement
- Fault – Sense of offset and kinematics unknown; dashed where approximately located, dotted where concealed
- Doughnut Formation basal detachment fault – Dashed where approximately located, arrows show relative direction of displacement on cross sections
- Lacustrine shorelines – Major shorelines of Lake Bonneville, Gilbert-episode lake, and Great Salt Lake; mapped at the top of wave-cut bench for erosional shorelines and the top of constructional bars and barrier beaches; may coincide with geologic contacts; dashed where approximately located:
  - S Lake Bonneville, Stansbury shoreline
  - B Lake Bonneville, Bonneville shoreline
  - t Lake Bonneville, transgressive shorelines (present above the Provo shoreline and below the Bonneville shoreline)
  - P Lake Bonneville, Provo shoreline
  - r Lake Bonneville, regressive shorelines (present below the Provo shoreline)
  - G Potential Gilbert-episode shoreline
  - Great Salt Lake, intermediate shoreline
  - H Great Salt Lake, Late Holocene highstand shoreline, dotted where concealed
  - h Great Salt Lake, historical highstand shoreline
  - Crest of lacustrine barrier bar or spit
- Outline of aggregate sand, gravel, and crushed stone quarry operations, contact based on 2011 and 2019 orthophotography (UGRC, 2011 and 2019)
- Bedrock and pre-disturbance surficial deposits are mapped in areas disturbed by aggregate mining operations in attempt to show the pre-mining geology and cross-cutting relationships
- A———A' Line of cross section
- Landslide or Lateral-spread scarp – Hachures on down-dropped side, dotted where concealed
- Lateral-spread hummock and depression – Hachures point in downslope direction
- 21 21 Strike and dip of inclined bedding– red symbols and text are from Van Horn (1981)
- Sand and gravel pit
- Abandoned sand and gravel pit
- Mine or quarry
- Abandoned mine or quarry
- Prospect
- Spring
- Selected water well
- Oil and gas exploration well, plugged and abandoned
- Rock sample location and number:
  - SLCN2014-283 Geochronology and geochemistry (McKean and Nevada Isotope Geochronology Laboratory, 2016; McKean, 2017)
  - SLCN2014-285 U-Pb zircon geochronology (McKean et al., 2016)
  - SLCN2014-284 Geochemistry (McKean, 2017)
- IA Paleoseismic trench (TF - Hylland et al., 2017; IA - Hiscock et al., 2023)
- Qlgp/Mg Stacked unit – Denotes thin cover of first unit overlying second unit

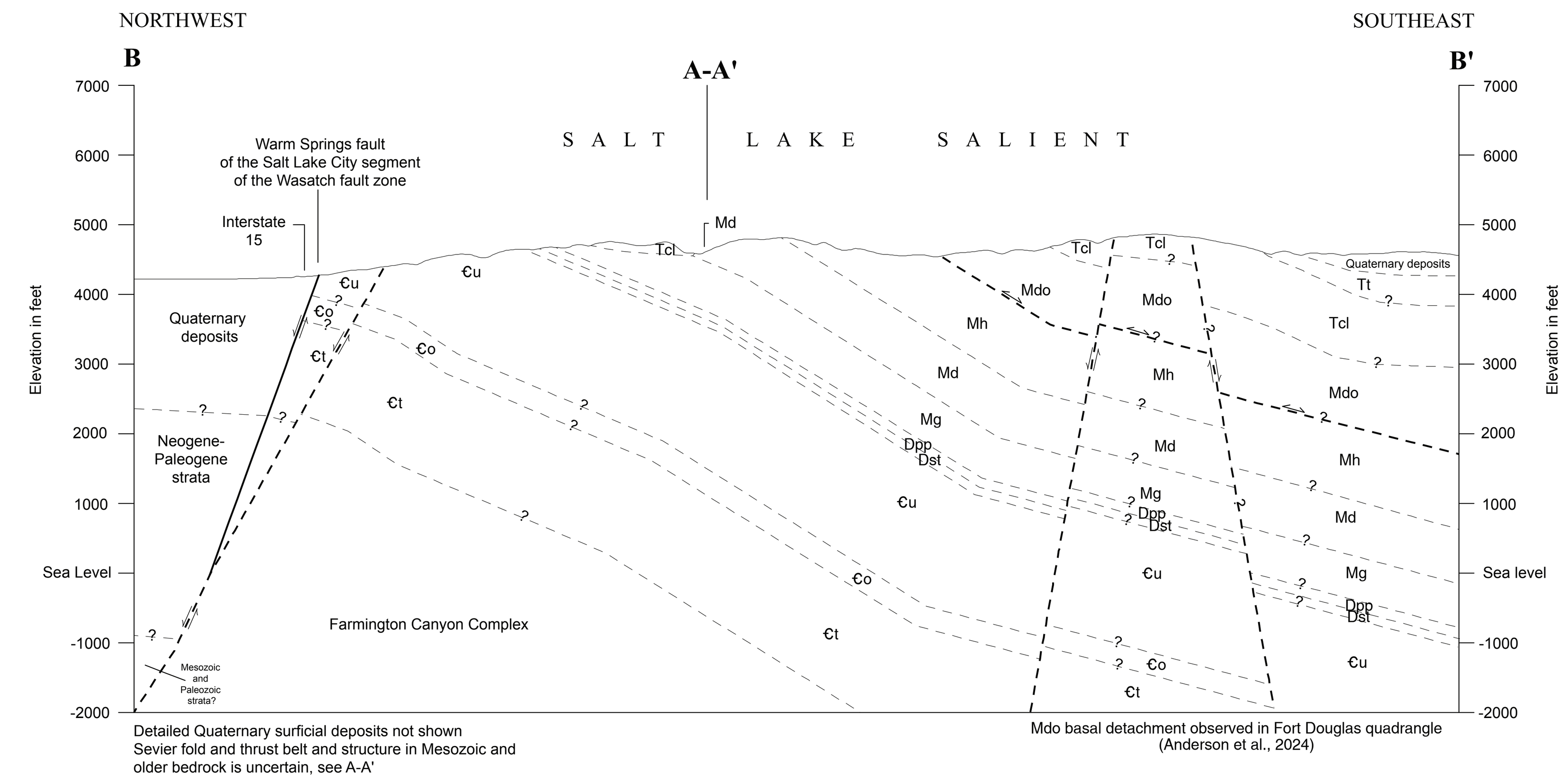

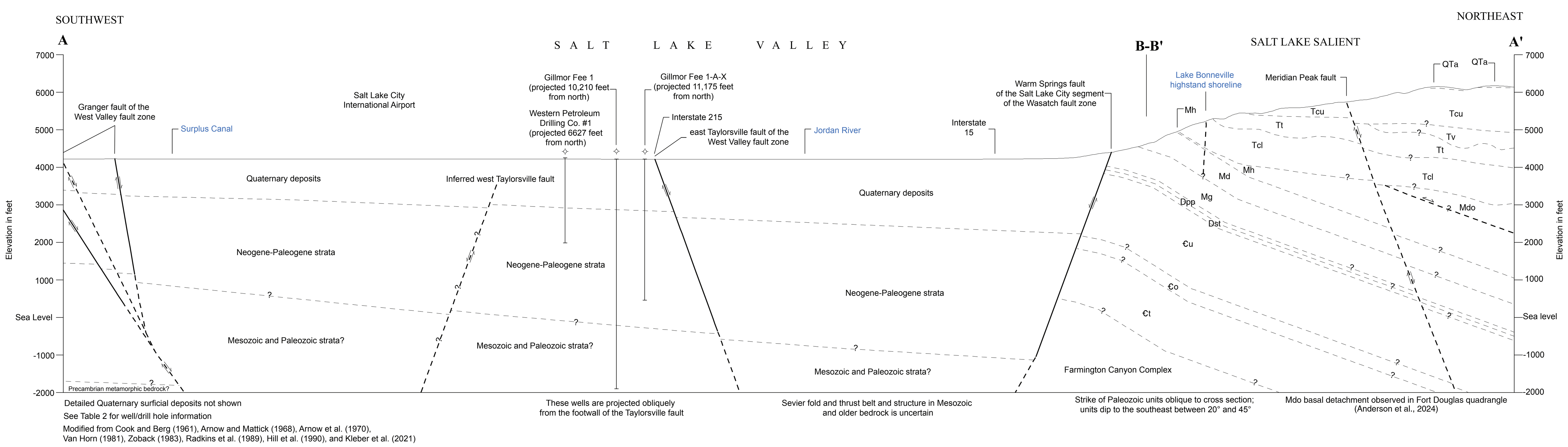

INTERIM GEOLOGIC MAP OF THE SALT LAKE CITY NORTH QUADRANGLE, SALT LAKE AND DAVIS COUNTIES, UTAH

by

Adam P. McKean and Zachary W. Anderson

Suggested citation:

McKean, A.P., and Anderson, Z.W., 2024, Interim geologic map of the Salt Lake City North quadrangle, Salt Lake and Davis Counties, Utah: Utah Geological Survey Open-File Report 768DM, 38 p., 2 plates, scale 1:24,000, https://doi.org/10.34191/OFR-768DM.

Disclaimer

This geologic map was funded by the Utah Geological Survey and the U.S. Geological Survey, National Cooperative Geologic Mapping Program, through USGS STATEMAP award number G13AC00169 (2013–2014). The views and conclusions contained in this document are those of the authors and should not be interpreted as necessarily representing the official policies, either expressed or implied, of the U.S. Government.

OPEN-FILE REPORT 768DM
UTAH GEOLOGICAL SURVEY
UTAH DEPARTMENT OF NATURAL RESOURCES
2024

INTRODUCTION

Location and Geography

The Salt Lake City North 7.5′ quadrangle is located in Salt Lake and Davis Counties from downtown Salt Lake City on the east to the Salt Lake International Airport on the west and extends north into Davis County to include the southern parts of the City of Bountiful and City of Woods Cross. The southern boundary of the quadrangle is at approximately 900 South Street in Salt Lake City. The quadrangle contains downtown Salt Lake City, the State Capitol building, the City of North Salt Lake, agricultural land, a number of oil refineries, a part of the Farmington Bay Waterfowl Management Area, and a number of wetlands. The Jordan River flows north through the center of the quadrangle towards Farmington Bay of Great Salt Lake. The eastern part of the quadrangle contains the western part of the Salt Lake salient, which forms an intermediate-elevation, east-west ridge between Salt Lake Valley and the Wasatch Range that separates Davis and Salt Lake Counties. City Creek flows from the Wasatch Range and empties into the valley in the southeast corner of the quadrangle. The western part of the quadrangle contains Great Salt Lake wetlands and mudflats, and the alluvial plain and deltas of the Jordan River. This project will provide the basis for identifying and delimiting potential geologic hazards in future Utah Geological Survey (UGS) derivative geologic hazard maps, part of the UGS Geologic Hazards Mapping Initiative (Christenson and Ashland, 2007; Castleton and McKean, 2012).

GEOLOGY

Geologic Structure

During the Paleo- to Mesoproterozoic, various geologic terranes were accreted to the North American Archean cratonic core, creating the basement rock for this region (Nelson et al., 2002; Dickinson, 2006; Whitmeyer and Karlstrom, 2007). This basement bedrock is not exposed in the quadrangle but likely underlies the quadrangle and is exposed to the north in the Farmington Canyon Complex and on Antelope Island (see Hedge et al., 1983; Bryant, 1988, 1990; Doelling et al., 1990; Yonkee et al., 2000; Willis et al., 2010; Anderson, 2023).

Regionally, the area developed east-directed thrust faults and folds during largely contractional tectonism of the Cretaceous to Paleogene Sevier orogeny (DeCelles, 2004; Yonkee and Weil, 2015). Paleozoic rocks in the map area are autochthonous to the Willard thrust fault and are part of a large southeast-dipping panel of rocks in the north limb of the Emigration Canyon syncline (Bryant, 1990; Yonkee and Barnett, 2000; Yonkee and Weil, 2011; Coogan and King, 2016; Clark et al., 2020). Bedding parallel detachment horizons that likely accommodated east-directed thrusting are hypothesized to be present in the lower part of the undivided Cambrian unit and near the base of the Mississippian Doughnut Formation (see cross section B–B’ on Plate 2), but poor exposures and aggregate mining operations preclude any definitive observations of these faults. Contraction ceased and orogenic collapse dominated during most of the Paleogene (Constenius, 1996). Plate boundary reorganization along the western margin of North America eventually led to continental extension manifested by Basin and Range extensional faulting that began in the area about 18 Ma and continues today (Parry and Bruhn, 1986). The Wasatch fault zone is a major segmented normal fault zone that bounds the east side of the Basin and Range Province and creates the stark topographic rise of the Wasatch Range in its footwall to the east and the relatively flat valley bottoms in its hanging wall to the west (Gilbert, 1928; Cluff et al., 1970; Machette et al., 1992). The Salt Lake salient is a fault-bounded bedrock block that structurally defines the overlapping and complicated boundary between the Salt Lake and Weber fault segments (Personius and Scott, 1992). Parts of the Weber and Salt Lake segments of the Wasatch fault zone bound and cut the Salt Lake salient in the eastern part of the map. The West Valley fault zone is present in the southwestern part of the map and is largely antithetic to the Wasatch fault zone. These faults and other geologic hazards are described and discussed in more detail in the Surface Fault Rupture subsection of the Selected Geologic Hazards section.

Bedrock Stratigraphy

Paleozoic and Paleogene bedrock are exposed in the east part of the quadrangle in the Salt Lake salient fault block. In the adjacent Fort Douglas quadrangle to the east, the Paleoproterozoic Farmington Canyon Complex is overlain by Early to Middle Cambrian Tintic Quartzite and Ophir Formation. Although these units are not exposed in the quadrangle, we expect they underlie the Salt Lake salient and are faulted down in Salt Lake Valley (Van Horn and Crittenden, 1987; Bryant, 1988; Anderson, 2023; Anderson et al., 2024). The oldest map unit exposed in the quadrangle is the Middle to Late undivided Cambrian rocks (Ꞓu) which are fractured and altered limestone, dolomite, and shale of the Maxfield Limestone, Bloomington Formation, Nounan Formation, and St. Charles Formation. The Lower Cambrian strata are unconformably overlain by Late Devonian through Mississippian strata. The Devonian through Late Mississippian strata are marine carbonates and clastics including the Stansbury Formation (Dst), Pinyon Peak Limestone (Dpp), Gardison Limestone (Mg), Deseret Limestone (Md), Humbug Formation (Mh), and Doughnut Formation (Mdo).

An angular unconformity between Paleozoic and Paleogene rocks is marked by a prominent "terra rosa" or red-weathering paleosol, developed potentially during or just after the Sevier-age thrusting and erosion. Paleogene strata include, in ascending order, a lower conglomerate (Tcl); mixed clastic and tuffaceous strata (Tt) that include conglomerates, sandy limestone, sandstone, and mudstone, all with a varying tuffaceous component; a volcaniclastic conglomerate (Tv); an upper conglomerate (Tcu); and older alluvial deposits (QTa). Disconformities, some with angular discordance, separate each unit. A detrital zircon U-Pb age from the top of Tcl indicates a maximum depositional age of 48.47 ± 0.76 Ma (McKean et al., 2016), suggesting these rocks may correlate with the Late Paleocene to Early Eocene Wasatch Formation exposed to the east (Bryant, 1990). Strata in Tcl and parts of Tt likely represent deposition of synorogenic alluvial material deposited in wedge-top basins of the Sevier thrust belt (Yonkee et al., 1997; Yonkee and Weil, 2011). A detrital zircon U-Pb age of 44.75 ± 0.29 Ma from Tt and an $^{40}Ar/^{39}Ar$ age of 39.52 ± 0.19 Ma from Tv corroborate previous studies that yielded Middle Eocene ages from the same units (McKean et al., 2016; McKean and Nevada Isotope Geochronology Laboratory [NIGL], 2016). These rocks could be associated with orogenic collapse in the area that began during the Eocene (Constenius, 1996). Igneous activity in the region contributed material to units Tt and Tv (see Best and Christiansen, 1991; and Clark et al., 2020 and references therein). An apatite (U-Th)/He age of 36.5 ± 5.1 Ma (Armstrong et al., 2004) from Tv in the Salt Lake salient indicates that since the Paleogene, the unit was not buried deep enough during extensional collapse and Basin and Range normal faulting to reset the He ages. The upper conglomerate unit (Tcu) reflects a tectonic setting of continued orogenic collapse, local drainage reversal, and a source area that tapped local Paleozoic rocks and areas of uplifted Tcl or Wasatch Formation during the Oligocene (Mann, 1974; Constenius, 1996; Anderson and McKean, 2018). Detrital zircon U-Pb age data show that Tcu contains sparse Cenozoic zircons and potentially indicate a maximum depositional age of Early Oligocene (Anderson and McKean, 2018). The lack of Miocene zircon grains in Tcu (which are abundant in the Middle Miocene to Pliocene Salt Lake Formation in the surrounding area) and dips up to ~30° suggest that Tcu is likely Early Oligocene, possibly as young as Early Miocene (Anderson and McKean, 2018).

We assume that the old alluvial deposits (QTa) now stranded ~ 2000 feet (600 m) above the valley floor began to be uplifted and incised when the active movement of the Wasatch fault zone stepped westward from the Rudys Flat fault (to the east in the Fort Douglas quadrangle) to the Warm Springs fault (Anderson and McKean, 2018; Anderson et al., 2024).

Surficial Deposits

Surficial deposits within the quadrangle consist of alluvial, colluvial, lacustrine, marsh, mass-movement, and deltaic deposits. Lacustrine and deltaic sediments were deposited in Late Pleistocene Lake Bonneville (30 to 13 ka), the Gilbert-episode lake (~11.5 ka), and Holocene Great Salt Lake (since ~11 ka) (see Table 1, all ages are in calibrated years). Following Oviatt (2014), the Gilbert-episode lake is regarded as a separate lake, rather than a phase of the Bonneville or Great Salt Lake cycles. Along the range front, these lacustrine deposits interfinger with alluvial fans, fan-deltas, and colluvial deposits. During and since the regression of Lake Bonneville, the Jordan River has migrated across the valley floor depositing fluvial terraces, natural levees, point bars, and overbank deposits (see McKean and Hylland, 2019a, 2019b). Non-lacustrine surficial units in lower elevations (< 4230 feet [<1289 m]) may locally contain thin Great Salt Lake lacustrine sediments from periods of high lake elevation but were not mappable as a separate unit. Mass-movement deposits in the quadrangle include several historical landslides (Springhill, Parkway Drive, and City Creek landslides), older landslides, and liquefaction-induced lateral-spread deposits. A large post-Bonneville lateral spread complex in North Salt Lake and Woods Cross cities covers approximately 3.5 square miles (9.3 km^2) with different ages of movement separated by an internal contact. Other smaller lateral-spread deposits have been mapped in downtown Salt Lake City (Osmond et al., 1965; Van Horn, 1982; Van Horn and Crittenden, 1987). Loess is a component of many surficial deposits in the area but is variable and difficult to quantify without excavated exposures. In some exposures, a weak buried soil divides the loess into upper and lower parts. Optically stimulated luminescence (OSL) dating of upper and lower loess deposits exposed in a paleoseismic trench in the Baileys Lake quadrangle to the west yielded ages of 3.2 ± 0.5 ka and 12.5 ± 1.4 ka, respectively (Hylland et al., 2012, 2014). The loess in these trenches probably correlates with the loess observed in hand-dug auger holes in the map area. The presence of loess in the auger holes was used to distinguish between older deposits (Pleistocene to Early Holocene) that predate the loess and younger deposits (Middle and Late Holocene) that postdate the loess. On the Salt Lake salient, a geotechnical trench in the SE 1/4 of section 7, T. 2 N., R. 1 E. revealed over 10 feet (3 m) of continuous silt and clay deposits that we interpreted as thick loess deposits on the lee side of a ridge.

PREVIOUS MAPPING

Previous geologic maps of the area (Figure 1) include bedrock and surficial geologic maps of the quadrangle by Van Horn (1981, 1982) at 1:24,000 scale, and part of the quadrangle mapped by Van Horn and Crittenden (1987) at 1:24,000 scale. Other geologic maps of the area include Marsell and Threet's (1960) geologic map of Salt Lake County at approximately 1:63,360 scale, surficial mapping by Miller (1980) at 1:100,000 scale, and Bryant's (1990) Salt Lake City 30′ x 60′ quadrangle at 1:100,000 scale. Additional Wasatch fault zone and surficial mapping include Scott and Shroba (1985) and Personius and Scott (1992) at 1:50,000 scale, and Kaliser (1976) at approximately 1:150,000 scale.

Previous 1:24,000-scale mapping of the quadrangle by Van Horn (1981, 1982) includes surficial and bedrock geologic maps; however, these maps did not include the West Valley fault zone nor do they follow the UGS surficial mapping system (Doelling and Willis, 1995). Additional detailed mapping, at a scale of 1:24,000, is needed to define the extents of faults in the quadrangle, and to provide geologic information for planned geologic hazard maps (Bowman et al., 2009).

METHODS

Mapping of surficial deposits by the UGS is based on age and depositional environment or origin (Doelling and Willis, 1995). The letters of the map units indicate (1) age, (2) depositional environment or origin, determined from landform morphology, bedding, or other distinctive characteristics of the deposits, (3) grain size(s), and (4) age as related to the phases of Lake Bonneville. For example, unit Qal_1 is a Quaternary surficial deposit of alluvial origin (al), and the number one indicates it is young and potentially historically active. Letters "y" and "o" in place of a subscript indicate deposits younger and older than Lake Bonneville, respectively. Unit numbers indicate relative age with "1" being the youngest and increasing with age.

Mapping for the project was done on stereographic pairs of aerial photographs from the following sources: black-and-white aerial photographs from the U.S. Department of Agriculture (USDA) Agricultural Commodity Stabilization Service (1958) and Agricultural Stabilization and Conservation Service (1971), black-and-white aerial photographs from the USDA Agricultural Adjustment Administration (1937, 1946), black-and-white aerial photographs from the USDA Forest Service (1963), black-and-white oblique aerial photography at various scales from 1:12,000 to 1:5000 from the Woodward-Lundgren & Associates Wasatch fault investigation (Cluff et al., 1970, complied in Bowman et al., 2015), and natural color aerial photographs from the USDA National Agriculture Imagery Program (2009). Some contacts were chosen based on data from the U.S. Natural Resources Conservation Service (NRCS) (2010) soil map. Gravel pit outlines and some contacts were revised using 2011 and 2019 orthophotography (Utah Geospatial Resource Center [UGRC], 2011a and 2019). Most Quaternary-active faults, landslides, and some additional contacts were mapped using a variety of lidar elevation data (1- and 2-meter data available from UGRC [2006]; 1-meter data [UGRC, 2011b] and 0.5-meter data [UGRC, 2013–2014]). The geologic map was made by transferring the geology from the aerial photographs to a geographic information system (GIS) database using ArcGIS, VROne, and VRTwo software at a target scale of 1:24,000. Aerial-photographic and field mapping of the Salt Lake City North quadrangle was conducted by McKean in 2013–2014, with additional field work in 2018–2021 and 2023. Anderson conducted field mapping in 2016–2018 and 2021–2023.

In areas disturbed by aggregate mining operations, the surficial geology, bedrock geology, and Warm Springs fault traces show our interpretation of pre-mining geology and cross-cutting relationships. A pit extent outline and fill pattern indicates areas of land disturbed by quarrying (Plate 1). At the time this map was created, most evidence of faulting had been destroyed and most surficial deposits mapped in these areas had been removed by mining operations. Geology within the disturbed areas was interpreted using the pre-mining black-and-white aerial photographs (USDA, 1937), historical photographs, and drawings of the Warm Springs fault from Gilbert (1890).

Cross-sections A-A′ and B-B′ were created by combining available subsurface information and gravity data from several sources, including Cook and Berg (1961), Arnow and Mattick (1968), Arnow et al. (1970), Van Horn (1981), Zoback (1983), Radkins et al. (1989), Hill et al. (1990), and Kleber et al. (2021). Well logs (lithologic and electric) from exploration oil and gas wells (Table 2) were used in combination with the R-11 seismic line of Radkins et al. (1989) to help determine the subsurface contacts between unconsolidated Quaternary sediments, Neogene-Paleogene semi-consolidated strata, Mesozoic to Paleozoic consolidated bedrock, and Precambrian metamorphic bedrock (possibly Precambrian Farmington Canyon Complex) (see Subsurface Units section for more information).

SELECTED GEOLOGIC HAZARDS

Geologic hazards identified in this area include surface fault rupture, landsliding, rockfall, debris flow, liquefaction-induced lateral spread, and flooding. Other potential geologic hazards could include expansive soils, collapsible soils, corrosive soils, other problem soils, shallow groundwater, and earthquake-induced ground shaking, liquefaction, tectonic subsidence/tilting, tsunami or seiche waves, and flooding associated with earthquakes. Spring and marsh deposits (Qsm, Qam, and Qlam) in areas of shallow groundwater and clay-rich lacustrine deposits may also cause soil problems.

Below is a discussion of the known landslides, rockfalls, active faults, and climate-related lake-flooding in the quadrangle. See the map unit descriptions and geologic map (Plate 1) for more information and locations of these features. Additional geologic hazards may exist, like those listed above, and are not addressed in this report. For a comprehensive geologic hazards assessment of any property, we recommend site-specific geotechnical and geologic hazard investigations per the guidelines in UGS Circular 128 (Bowman and Lund, 2020). See the UGS website (https://geology.utah.gov) for additional information regarding geologic hazards.

Landslides

In the Salt Lake City North quadrangle, numerous landslides are active or have shown evidence of historical movement (Qmsh), based on written or verbal accounts of movement, as observed by UGS geologists during mapping, or where movement is detectible between different ages of aerial photographs ranging from 1977, mid-1990s, and 2011 (UGRC, 1977, mid-1990s, 2011a). A brief description of the historically active Springhill, City Creek, and Parkway Drive landslides that have been monitored by the UGS Geologic Hazards Program is provided below. Other landslides within the quadrangle, including numerous smaller landslides with historical movement, are included on Plate 1 and discussed in the Description of Map Units section below. Areas of landsliding are common on slopes that contain Lake Bonneville lacustrine units overlying, or within exposures of, Paleogene tuffaceous strata (Tt) and volcaniclastic conglomerate (Tv). Landslides with subdued morphology (suggesting that they are older, weathered, and have not moved recently) may continue to exhibit slow creep or are capable of renewed movement if stability thresholds are exceeded (Ashland, 2003). Age and stability determinations require detailed geotechnical investigations. Numerous liquefaction-induced lateral spread deposits are mapped in the quadrangle (Qml and Qml_3), including the large North Salt Lake lateral spread (Harty and Lowe, 2003); see the Description of Map Units for more information on this type of geologic hazard.

The Springhill landslide is a slow-moving landslide that has gradually distressed and destroyed homes and infrastructure between Valley View Drive and Springhill Drive in North Salt Lake (NW ¼, section 12, T. 1 N., R. 1 W.) since the late 1990s (Giraud, 1999). At the time of this report, 17 homes have been destroyed or demolished because of the landslide and the area has been converted to city-owned open space (McKean et al., 2012; UGS, 2012). The landslide is composed of Lake Bonneville lacustrine gravel deposits (Qlgp), former aggregate-mining fill, and weathered Paleogene tuffaceous strata (Tt) and volcaniclastic conglomerate (Tv). Shallow groundwater and several springs and seeps are present in the landslide. The toe of the landslide crosses the Warm Springs fault of the Wasatch fault zone.

The City Creek landslide is on the northern slope of City Creek Canyon between the drainage bottom and East Capitol Boulevard (east half of section 30, T.1 N, R. 1 E.). Movement was reported in May 1998 (Ashland, 2003) and has continued to move since then. The landslide was active before 1998 with movement predating USDA 1937 aerial photographs. Lake Bonneville fine-grained deposits (Qad) are exposed in the main scarp and are underlain by Paleogene tuffaceous strata (Qlgb/Tt) and potentially volcaniclastic conglomerate (Tv). Numerous historically active smaller landslides occupy the surrounding slopes.

During this project, the Parkway Drive landslide, in the North Salt Lake's Eaglepointe subdivision (boundary of sections 12 and 13, T. 1 N., R. 1 W.), moved on August 5, 2014. The landslide failed along a north-facing wall of a reclaimed aggregate pit cut in the 1990s (UGS, undated) that had a small shallow landslide in the mid-2000s. The landslide is composed of Lake Bonneville lacustrine gravel and sand deposits (Qlgb) and weathered Paleogene tuffaceous strata (Tt) (UGS, undated; Hill, 2018). One home was destroyed, and some commercial tennis court structures were damaged.

Rockfall

Rockfall hazard in the Salt Lake City North quadrangle is significant. Although only one deposit of talus (Qmt) was large enough to include on the map (SE1/4 of section 19, T.1 N, R. 1 E.), the factors that may contribute to rockfall hazard are present in numerous locations on and around the Salt Lake salient. Several bedrock units form cliffs and steep slopes above

Lake Bonneville shorelines, including the Paleogene upper and lower conglomerate (Tcl and Tcu). In areas near faults, these rocks are commonly fractured, which can enhance mechanical weathering and create a potential source for rockfall. A rockfall occurred on the slope above Oak Forest Road in Salt Lake City (section 19, T. 1 N., R. 1 E.) on April 17 or 18, 1999 (Rich Giraud, UGS, verbal communication, 2013). Fractures are visible in the overlying cliffs composed of Paleogene upper conglomerate (Tcu) bedrock, and future rockfall may occur in the immediate area. Stability determinations and mitigation recommendations require detailed geotechnical investigations.

Great Salt Lake and Flooding

Historic highstands of Great Salt Lake occurred in the late 1860s to early 1870s and again in 1986–87, with water reaching a maximum still water elevation of 4212 feet (1284 m) (Arnow and Stephens, 1990) and superelevation between 4211 and 4223 feet (1832–1287 m) on nearby Antelope Island (Atwood, 2006). A lake-level rise to the historic highstand shoreline could potentially flood much of the low-elevation valley floor in the quadrangle and elevate shallow groundwater in the area, as was observed in the 1980s (Harty and Christenson, 1988; Hecker et al., 1988; Arnow and Stephens, 1990). Additionally, land above the historic highstand elevation could be affected by elevated shallow groundwater levels and potential storm wave run-up along the shoreline, as was documented following the 1980's historic highstand (Atwood and Mabey, 1995; Atwood, 2006). Recommendations were made during the last historic highstand that development surrounding Great Salt Lake should be restricted below the elevation of 4217 feet (Utah Division of Comprehensive Emergency Management, 1985, in Harty and Christenson, 1988).

Flooding due to earthquake related tectonic subsidence/tilting (see Keaton, 1987; McKean and Hylland, 2019b) and tsunami or seiche waves (see Francis et al., 2011) are a concern around the shore of Great Salt Lake and the Jordan River.

Surface Fault Rupture

Active faults pose a major threat to residents of the Wasatch Front (Earthquake Engineering Research Institute, Utah Chapter, 2015) for earthquake ground shaking, surface rupture, liquefaction, lateral-spread, and other shaking related effects and have long been the focus of geological mapping and hazard investigations in the area (see, for example: Gilbert, 1890; Marsell and Threet, 1960; Kaliser, 1976; Miller, 1980; Scott and Shroba, 1985; Personius and Scott, 1992; Gori and Hays, 1992; Lund, 2005; DuRoss et al., 2014; DuRoss et al., 2016; McDonald et al., 2020; Liberty et al., 2021). One of the goals of this mapping was to identify the location of Quaternary-active faults in the quadrangle. Four Holocene-active faults are recognized in the quadrangle: (1) the Warm Springs fault of the Salt Lake City segment of the Wasatch fault zone, (2) the Weber segment of the Wasatch fault zone, and (3 & 4) the Granger and Taylorsville faults of the West Valley fault zone. Additional faults in the Salt Lake salient are also hypothesized to be Quaternary active but may not have experienced slip during the Holocene. Fault names in this section follow the U.S. Geological Survey Quaternary Fault and Fold Database of the United States fault hierarchy terminology from larger to smaller divisions: section or segment, fault zone, fault, and strand (see https://www.usgs.gov/programs/earthquake-hazards/faults).

Warm Springs fault

The Warm Springs fault of the Salt Lake City segment of the Wasatch fault zone is a down-to-the-west normal fault, bounding the western part of the Salt Lake salient and extending into the Salt Lake Valley. Here, we describe the northern, central, and southern parts of the Warm Springs fault as shown in Figure 2. These parts are broken out based solely on map pattern and are used to clarify the discussion regarding certain parts of the fault.

On March 18, 2020, the M_w 5.7 Magna earthquake occurred, the hypocenter of which was in the adjacent Magna quadrangle to the southwest. Numerous aftershocks followed with hypocenters in the newly mapped Saltair graben and West Valley fault zone, including some within the Salt Lake City North quadrangle (Pang et al., 2020; Kleber et al., 2021). Seismologic and structural analysis from Kleber et al. (2021) and Pang et al. (2020) suggested a hypothetical structural model that identified a listric Warm Springs fault as the causative fault for the earthquake, or a fault like it in the hanging wall of the Wasatch fault zone.

Northern part of the Warm Springs fault: We define the northern part of the Warm Springs fault from where the fault splits in section 11, T. 1 N., R 1 W. north to Bountiful and Woods Cross. We have identified and mapped two strands: an eastern and western strand (Figure 2a).

Northern part, eastern strand: The eastern strand wraps around the northern part of the Salt Lake salient and generally trends northeast-southwest. Many of the Holocene scarps of this strand have been obliterated by aggregate mining operations and urban development, but the 1937 and 1958 aerial photographs clearly show fault scarps cutting Holocene and Pleistocene deposits along the mapped length of this strand. Our mapping generally follows that of Van Horn (1981, 1982) and includes splays and a north-south-trending strand mapped in the NE ¼ of section 1, T. 1 N., R. 1 W. Personius and Scott (1992) interpreted the northern part of this strand as a shoreline and mapped small segments of more northerly trending faults that we did not see evidence for. A consultant's surface fault rupture trench investigation confirmed the location of the eastern trace of the Warm Springs fault just northeast of the Springhill landslide (Applied Geotechnical Engineering Consultants, Inc., 1994) along 100 South and Cynthia Way in North Salt Lake (see NSL3 Figure 2a; NW ¼, NE ¼, section 12, T. 1 N., R 1 W.). This strand parallels, overlaps, and is about 0.8 miles (1.2 km) west of the southern end of the Weber segment of the Wasatch fault zone. The geometry and proximity of the northeastern Warm Springs fault suggests that it may be more kinematically related to the southern Weber segment than the Salt Lake City segment of the Wasatch fault zone.

Northern part, western strand: The western strand of the northern part of the Warm Springs fault trends north-northeast and is separated from the topographic escarpment of the Salt Lake salient (sections 26 and 35, T. 2 N. R. 1 W., and section 2 and 11, T. 1 N., R 1 W.). Although most surficial evidence of this fault is now destroyed by urban development, a clear west-facing topographic escarpment is present on the 1937 aerial photographs. However, the origin and nature of this escarpment has been disputed in the past and as a result is mapped as a queried fault. Previous interpretations are a fault, a shoreline, or an escarpment associated with a liquefaction-induced lateral-spread landslide. Van Horn (1982) interpreted this feature as a fault cutting mostly lateral-spread deposits and mapped its 4-mile-long (6.5 km) trace along a 20-foot-high (6 m) topographic escarpment at approximately the 4250-foot (1295 m) elevation contour. Personius and Scott (1992) interpreted this feature to be the Gilbert-episode lake highstand shoreline (using terminology after Oviatt [2014]). Robison et al. (1991) conducted a geotechnical investigation of the escarpment using trenching and correlation of geologic units across boreholes. The northern borehole and trench site were perpendicular to the escarpment at about 700 North and 400 West in North Salt Lake City (see NSL1 Figure 2a; NW ¼, NE ¼, section 2, T. 1 N., R. 1 W.) and the other borehole study was located near the interchange of Interstates 15 and 215 (see NSL2 Figure 2a). The trenching showed shallow listric slumping or faulting and the borehole study showed continuous and undeformed deep-water lacustrine sediments beneath the listric faults or slumping. Robison et al. (1991) concluded that the escarpment was not formed by tectonic faulting but was likely the result of lateral-spread landsliding and possibly gravitational slumping adjacent to the Gilbert-episode lake highstand shoreline. However, several other observations suggest that the scarp may be the Warm Springs fault. First, the scarp cuts both liquefaction-induced lateral-spread deposits (Qml_3) and fine-grained Lake Bonneville lacustrine sediments (Qlf) beyond the lateral-spread deposits and thus may not be solely explained as a lateral-spread feature. Second, while this feature is at the correct elevation for the Gilbert-episode lake highstand shoreline, the scarp height of 10 to 20 feet (3–6 m) is larger than Gilbert-episode lake shoreline escarpments exposed elsewhere in the quadrangle and surrounding areas. We suggest this may be a shoreline that has been controlled and enhanced by a tectonic fault. Third, the scarp has a nearly continuous north-northeast linear trend for approximately 4 miles (6.5 km) and lacks the expected curved shape typical of a lateral spread scarp. Rather, the geometry fits better to potentially be part of a zone of en echelon faults near the southern end of the Weber segment of the Wasatch fault zone. Fourth, Cook and Berg's (1961) gravity measurements in the area identified a basin graben in the area and mapped the eastern bounding down-to-the-west fault of the graben near where we map this fault strand. However, in light of the borehole evidence from Robison et al. (1991), it is also possible that this feature may be part of a lateral-spread scarp combined with a tectonic fault scarp, which may have later impeded and was modified by the Gilbert-episode lake shoreline. There are conflicting interpretations of this feature, but we choose to map it as a queried fault and a shoreline.

Central part of the Warm Springs fault: We define the central part of the Warm Springs fault where the fault is a single strand between NE ¼ section 14, T. 1 N., R. 1 W. south to where the fault bifurcates in N 1/2 section 25, T. 1 N., R. 1 W. (Figure 2b). Surficial expression of the central part of the fault has mostly been removed by aggregate mining operations and industrial development but the surficial geology, bedrock geology, and Warm Springs fault traces are shown as our interpretation of pre-mining geology and cross-cutting relationships. Along North Beck Street, previous maps placed the Warm Springs fault in approximately the same position near the base of the bedrock face, as such this fault trace is not included on Figure 2 (Marsell and Threet, 1960; Kaliser, 1976; Miller, 1980; Van Horn, 1981, 1982; Scott and Shroba, 1985; Bryant, 1990; Personius and Scott, 1992), where USDA (1937) aerial photographs show pre-excavation evidence of normal faults offsetting alluvial and lacustrine deposits. Before development and mining obscured most geologic relationships, Gilbert (1890, p. 348, and Plate XLIV) described and W.H. Holmes sketched multiple fault scarps cutting a Holocene alluvial fan near Jones Canyon (SW ¼, section 24, T. 1 N., R. 1 W.). During field work in 2013, we observed exposures of the bedrock footwall and slickensides of the fault in quarries, but the hanging wall of the fault had been mostly removed by mining activities.

Southern part of the Warm Springs fault: We define the southern part of the Warm Springs fault as south of the point at which the fault bifurcates, south of N 1/2 section 25, T. 1 N., R. 1 W., near the mouth of Hell Canyon, to its southern mapped extent. Holocene fault scarps along this part of the fault have been almost completely obliterated or obscured by aggregate mining or urban development, making identification and mapping of the fault difficult and a topic of debate. Several differing interpretations of the location and extent of this part of the Warm Springs fault have been proposed including whether there are one or two strands of this fault (Figure 2b). Similar to Marsell and Threet (1960) and Scott and Shroba (1985), we have identified two main strands of this part of the fault, here discussed as eastern and western strands (similar to faults A and B of Scott and Shroba [1985], respectively; Figure 2b), along with a short northeast-southwest-trending fault near Washington Elementary School that connects the two strands. In 2015–2016 and 2017–2018, Dr. Lee Liberty of Boise State University conducted shallow seismic surveys in the downtown region of Salt Lake City, which will be discussed in the sections below (Liberty, 2016, 2018; Liberty et al., 2021). The following paragraphs describe locations, systematically from north to south, and methods by which we and previous workers have identified these parts of the Warm Springs fault.

<u>Southern part, eastern strand:</u> The eastern strand of the southern part of the Warm Springs fault is similar to Scott and Shroba's fault A and Kaliser's (1976) mapping of the Warm Springs fault (Figure 2b). Liberty et al. (2021) confirmed the existence and location of a fault between North Wall Street and North West Capitol Street on West Girard Avenue where seismic images show surficial deposits offset against shallow bedrock, which we interpret as the eastern strand. A review of aerial photographs, topographic data, and records in the UGS GeoData Archive (https://geodata.geology.utah.gov, includes consultant surface fault rupture investigations and UGS excavation reports) found no evidence for the continuation of the eastern strand south of 300 North Street (Figure 2b). However, Liberty et al. (2021) identified several potentially concealed faults that may represent a southern continuation of fault A into downtown Salt Lake City, but more work is needed to confirm if the faults connect to the eastern strand or are a distributed zone of faulting.

<u>Southern part, connecting strand:</u> A consultant's trench investigation at the Washington Elementary School (see WES on Figure 2b) identified part of the Warm Springs fault near 400 North and 200 West (Sergent, Hauskins & Beckwith, 1991). Although the geologic deposits on either side of the fault could not be directly correlated, there is at least 40 feet (12 m) of cumulative surface displacement across the fault at the site. During the construction of a new retaining wall at Washington Elementary School in 2020, the fault was exposed along the east side of the school grounds. UGS geologists observed the fault and surficial sediments and collected OSL samples to bracket the age of deformation. However, those samples have not been analyzed and are awaiting funding at the time of writing this report. The faulting identified by Sergent, Hauskins & Beckwith (1991) and confirmed by the authors in 2020, is a previously unmapped down-to-the-northwest normal fault that links the eastern and western strands. The fault also forms an observable scarp in high-resolution lidar data (UGRC, 2013–2014). Liberty et al. (2021) identified several faults near Washington Elementary School that could be the connecting strand or a series of distributed faults between the eastern and western strands.

<u>Southern part, western strand:</u> The queried northern part of the western strand, just south of the bifurcation point, appears to cut and offset an alluvial fan (Qafy) in the 1937 aerial photographs (USDA, 1937). Continuing south of Beck Street (SR 89) and west of 300 West Street, the fault scarp in 1937 aerial photographs (USDA, 1937) appears to closely coincide with a suspected Gilbert-episode lake shoreline (Plate 1). On the west side of 300 West, between 800 North and Reed Avenue, a cone penetrometer test (CPT) discovered a fault with 6 to 7 feet (1.8–2.1 m) of vertical, down-to-the-west displacement (see CPT on Figure 2b; David Simon, Simon Bymaster, Inc., written communication, 2014), which we interpret to be the western strand of the Warm Springs fault. Between 800 North and 300 North, the strand approximately coincides with a topographic escarpment on the 1934 topographic map (USGS, 1934). Farther south, between 300 North and North Temple, Liberty et al.'s (2021) shallow seismic work identified several faults and potential lateral-spread deposits that parallel and likely are related to the western strand. This western strand of the fault is mapped as queried due to the uncertainty of the combined observations.

During the Salt Palace Convention Center expansion project (near 200 South and between 200 West and West Temple, see SPCC on Figure 2b) in the late 1990s, grabens were discovered within the construction footprint by geotechnical investigations (Kleinfelder, Inc., 1999; Simon Bymaster, Inc., 1999). The investigations gave conflicting interpretations of the observed deformation, where Simon Bymaster, Inc. (1999) interpreted the features as tectonic faulting and Kleinfelder, Inc. (1999) interpreted them as liquefaction-induced lateral spreading. Liberty et al.'s (2021) shallow seismic survey identified a fault near our shorter western graben fault, as well as lateral spreading in this area. Drawing on observations from Liberty et al. (2021) and valid aspects of the two previous geotechnical investigations (Kleinfelder, Inc., 1999; Simon Bymaster, Inc., 1999), we chose to show both tectonic faults and lateral-spread deposits (Qafy/Qml) on Plate 1 in this area.

Liquefaction features and a small graben were identified at the Rose Wagner Theater expansion project (150 West Broadway [300 South], see RWT on Figure 2b) and were interpreted as a liquefaction-induced lateral spread by AGEC (1999). Due to the recent data brought forth by Liberty et al. (2021) immediately to the north at the Salt Palace Convention Center, we continue both the lateral spread and tectonic faults to this location (Plate 1).

Farther south, a cone penetrometer test by Leeflang (2008) along 400 South between 425 West and 225 East, found evidence for tectonic faulting between 200 West and State Street. Their data between 130 West and 56 West show a fault with approximately 8.7 meters (28.5 feet) of vertical offset of subsurface Late Pleistocene lacustrine and alluvial deposits. Between 56 West and 29 East, a second fault with a vertical offset of approximately 3 m (~10 feet) was identified from the same CPT line of borings. Their interpreted faults are significant and provide additional support for continuing the western strand to at least 400 South.

Liberty et al.'s (2021) seismic surveys along 700 South and 800 South Streets identified faults near the intersections with West Temple Street. We hypothesize that these concealed faults are the southern continuation of the western strand of the Warm Springs fault, but more work is needed to confirm if the faults connect to the western strand or if they represent a distributed zone of faulting.

Liberty et al. (2021) identified a broad zone of deformation (faulting and folding) in the subsurface of Salt Lake City between the Warm Springs and East Bench faults (see McKean, 2020; and McDonald et al., 2020 for location of East Bench fault) that they interpreted as a relay ramp system between the two faults. This deformation zone becomes more diffuse near the southern mapped extent of the Warm Springs fault (see Figure 2 and 5 of Liberty et al., 2021). How these seismically identified faults and folds connect to previously mapped fault strands, to each other, or if they represent a more diffuse zone of deformation between the Warm Springs and East Bench fault needs more work.

West Valley Fault Zone

The West Valley fault zone is composed of the Granger (western faults) and Taylorsville (eastern faults) fault sections that are partially antithetic to the Salt Lake City segment of the Wasatch fault zone. The West Valley and Wasatch fault zones bound an intrabasin graben in the quadrangle. The West Valley fault zone was first mapped by Marsell and Threet (1960). Cook and Berg (1961) correlated the Granger fault section to a steep gravity gradient in what they called the Jordan Valley graben. Marine and Price (1964) named the faults the Granger and Taylorsville faults of the Jordan Valley fault zone and provided drill-hole data for displacement minimums across the faults. Van Horn (1979 and 1982) did not show the fault zone: he attributed the scarps to differential erosion of distinct stratigraphic units (Van Horn, 1986, personal communication in Keaton et al., 1987). Miller (1980) included the northern part of the Granger fault on his map but attributed the lines as scarps with uncertain origin. Keaton et al. (1987) and Keaton and Currey (1989) conducted the first detailed investigations of the fault zone and confirmed, through geomorphic mapping, surface fault rupture investigations, paleoseismic trenches, and borings, the existence of the Granger and Taylorsville faults. They retained the existing Granger and Taylorsville fault names but proposed the two faults together be called West Valley fault zone.

Only a few paleoseismic investigations (Keaton et al., 1987; Keaton and Currey, 1989; Hylland et al., 2014, 2022; discussed below) have been performed on the fault zone, mainly because development has obscured the scarps and prevented excavation of paleoseismic trenches. However, combined West Valley fault zone paleoseismic data show four Middle to Late Holocene earthquakes that have mean modeled ages coincident with earthquakes on the Salt Lake City segment and the Weber segment of the Wasatch fault zone (Hylland et al., 2022), which support the hypothesis that the West Valley fault zone moves coseismically with, or has faulting triggered by, earthquakes on the Salt Lake City or Weber segments of the Wasatch fault zone (see DuRoss and Hylland, 2015; Hylland et al., 2022). An aftershock cluster related to the March 18, 2020, M_w 5.7 Magna earthquake occurred within the vicinity of the modeled subsurface intersection of the West Valley fault zone with the Warm Springs fault (Kleber et al., 2021; Pang et al., 2020). These new observations corroborate the paleoseismic research of DuRoss and Hylland (2015) and Hylland et al. (2022) noted above.

Granger fault: The western faults of the West Valley fault zone are called the Granger fault and are a series of down-to-the-east normal faults. The length of the Granger fault section is approximately 11.5 miles (~18.5 km) and is discontinuously exposed in this quadrangle, and in the Baileys Lake and Salt Lake City South quadrangles (McKean, 2019b; McKean and Hylland, 2019a).

Keaton and Currey's (1989) study of the West Valley fault zone included two localities within the quadrangle (Three Flags locality at SW 1/4, SE 1/4, NW 1/4, section 6, T. 1 S., R. 1 W. and Goggin Drain locality at SW 1/4, SE 1/4, NE 1/4, section 6, T. 1 S., R 1 W.).

At the Three Flags study site, borehole data documented monoclinal folding, suggesting that at least one earthquake had offset post-Lake Bonneville sediments. At the Goggin Drain study site, borehole data indicated 5 feet (1.5 m) of post-Lake Bonneville offset and up to 12 feet (3.6 m) of offset of pre-Lake Bonneville sediments.

A paleoseismic investigation in the adjacent Baileys Lake quadrangle revealed that this part of the Granger fault is capable of surface-rupturing earthquakes that created 1- to 3-foot-high (0.4–1 m) fault scarps (Hylland et al., 2014). The investigation documented four large (surface-faulting) earthquakes since the highstand of Lake Bonneville (~18 ka, Table 1), the most recent having occurred about 5.5 ka.

Taylorsville fault: The eastern fault of the West Valley fault zone, the Taylorsville fault, extends north-south through the Salt Lake City North and Salt Lake City South quadrangles. The Taylorsville fault is approximately 9.7 miles (~15.6 km) long and is discontinuously exposed due to erosion and development. In the Salt Lake City North and Salt Lake City South quadrangle, the northern one-third of the Taylorsville fault has both down-to-the-east and down-to-the-west normal faults (McKean, 2019b). The southern two-thirds of the fault is down-to-the-east in the adjacent Salt Lake City South quadrangle (McKean, 2019b).

Several consultants' surface fault rupture trench investigations reported locating the Taylorsville fault in the quadrangle. An AGRA Earth & Environmental, Inc (1997) trench investigation documented surface faulting on the northernmost Taylorsville fault (NE 1/4, section 28, T. 1 N., R. 1 W., Plate 1). Two organic-rich, bulk-soil samples from these investigations (one of the samples was interpreted as scarp-derived colluvium) yielded an average calibrated age of 2.2 ka, which was interpreted as the approximate age of a surface-faulting earthquake by Solomon (1998). A trench investigation near 460 South Orange Street in Salt Lake City located a trace of the Taylorsville fault with about 24 inches (60 cm) of displacement and a small antithetic fault (Leeflang and Everitt, 1993). Just north of that site, surface-rupturing faults were found in a trench investigation at 270 South Orange Street (Mike Hylland, UGS, verbal communication, 2014).

Hylland et al. (2022) completed a paleoseismic trench investigation on the Taylorsville fault near the AGRA Earth and Environmental, Inc. (1997) trench site (see TF on Plate 1). Their study revealed evidence for three Late Holocene surface-faulting earthquakes. The depth of the trench was limited due to shallow groundwater, resulting in exposed deposits that were only as old as Middle Holocene. Hylland et al. (2022) constrained the youngest earthquake event to 0.4 ± 0.2 ka, the mean Late Holocene (post-2 ka) recurrence interval to 800 years, (open-interval) slip rates for the past ~2500 years as 0.2–0.4 mm/yr, and vertical slip rates for the past ~5000 years as 0.1–0.2 mm/yr.

The UGS recently completed paleoseismic trenching on the Taylorsville fault near Indiana Avenue and Interstate 215, near the southern boundary of the Salt Lake City North Quadrangle (see IA on Plate 1). Two parallel trenches were excavated in July 2022, across an approximately 5-foot-high (1.5-meter) west-dipping scarp. The depth of the trenches was limited due to shallow groundwater at the site, but preliminary results show evidence for potentially two surface-rupturing earthquakes (Hiscock et al., 2023).

Salt Lake salient

Several faults in the Salt Lake salient are Quaternary active, a few may even be Holocene active. Two of these faults are extensions of fault zones mapped in adjacent quadrangle areas: the Weber segment of the Wasatch fault zone from the north, and the Virginia Street fault from the east. The third fault in the quadrangle we discuss is the Meridian Peak fault on the ridge of the salient.

On the northside of the Salt Lake salient, the Weber segment overlaps with the northern part of the Warm Springs fault in the northeastern part of the quadrangle and in the northwestern part of Fort Douglas quadrangle (see mapping in McDonald et al., 2020; Anderson et al., 2024). Previous geologic maps of the area show a large, old landslide along the edge with the Fort Douglas quadrangle (section 7 and 18, T. 1 N., R. 1 E, Plate 1; Van Horn, 1982; Van Horn and Crittenden, 1987; Personius and Scott, 1992). Using high-resolution topographic imagery derived from lidar data, we mapped fault scarps of the Weber segment south to where they directly connect with the previously mapped landslide scarp, which we now interpret as a fault scarp. These new interpretations were also supported by field work and observation of consultant trenching in the area, which only revealed evidence for small local landslides, mixed colluvial and alluvial deposits, thick soils, and bedrock.

On the south side of the Salt Lake salient, the western end of the Virginia Street fault extends into the quadrangle. Strands of this fault are mostly concealed by Pleistocene and Holocene deposits except in City Creek Canyon, where two exposures were identified along Bonneville Boulevard, where the fault offsets tuffaceous sandstone and conglomerate next to Lake

Bonneville deposits, and in a road cut where Lake Bonneville gravels are offset. The fault also offsets Paleogene bedrock units near Ensign Peak and near the mouth of City Creek Canyon. These faults may be part of a larger fault zone bounding the eastern side of Salt Lake Valley called the Foothill fault in the Fort Douglas quadrangle, but more work is needed to understand the fault connections on the southside of the salient (McKean, 2020; Anderson et al., 2024).

Another fault with possible Quaternary movement is the Meridian Peak fault. The fault trends north-south across the salient ridgeline (Meridian Peak) entirely within the Paleogene Tcu unit. The fault has down-to-the-east scarps in Tcu that are visible in the topographic data, but it does not intersect any Quaternary deposits so relative age is difficult to determine. Based on the size and geomorphology of the scarp, we suspect the Meridian Peak fault is a Quaternary-active fault.

Near the mouth of City Creek Canyon, northeast-trending normal faults intersect with splaying normal faults of the western termination of the Virginia Street fault (Anderson et al., 2024). These intersecting faults create a complex pattern of bedrock outcrops. Most faults are largely concealed, which makes their location and orientation uncertain. No surface fault ruptures were observed in the Quaternary deposits. The most recent age of faulting may be within the Quaternary due to their assumed connection to the Virginia Street fault but could be older.

DESCRIPTION OF MAP UNITS

QUATERNARY

Alluvial Deposits

Qal_1 **Active stream and floodplain deposits (**Late Holocene) – Moderately to well-sorted, medium- to light-brown sand, gravel, silt, and minor clay; very fine to medium-grained sand; contains thin discontinuous sand lenses; rounded to angular sand grains; thin to medium bedded; sand grains are quartz, lithic fragments, and mica flakes; mapped in active channels, floodplains, and on minor terraces less than 5 feet (1.5 m) above creek and river channels along the Jordan River, City Creek, and North Canyon; along the Jordan River, the map pattern of this unit represents the alluvial channel before human modification; locally includes natural levees deposits and minor colluvial deposits along steep stream embankments; exposed thickness less than 15 feet (5 m).

Qaly **Young floodplain and stream deposits, undivided** (Holocene?) – Moderately sorted, light olive-gray to light brown sand, silt, and minor clay; very fine to medium-grained sand; contains thin discontinuous sand lenses; subangular to angular sand grains; thin to medium bedded; sand grains are quartz, lithic fragments, and mica flakes; locally contains gastropod shells and shell fragments; mapped along the Jordan River and paleo-Jordan River (McKean and Hylland, 2019a, 2019b) (concealed by the Salt Lake City International Airport) where the river incised through young lacustrine and deltaic deposits (Qldy), and where alluvial channels flowed north along the Granger and Taylorsville faults; mapped in abandoned meander channels, floodplains, and on minor terraces less than 5 feet (1.5 m) above active channels; locally includes a surficial loess veneer and minor colluvial deposits along steep stream embankments; locally may contain thin undifferentiated marsh and lacustrine deposits; includes both ages of younger stream deposits, where Qal_1 and Qal_2 deposits cannot be mapped separately, due to lack of bars and swales and because deposits are too small to show separately at map scale; includes alluvial deposits that may be older than the Gilbert-episode lake (Table 1), but postdates regression of Lake Bonneville from the Provo shoreline and lower shorelines; exposed thickness less than 15 feet (5 m).

Qatp **Stream terrace deposits, related to Provo shoreline and regressive phase of Lake Bonneville** (Late Pleistocene) – Moderately to poorly sorted pebble and cobble gravel with a matrix of sand, silt, and minor clay; subangular to rounded clasts; mapped in one location on a terrace 200 to 240 feet (60–73 m) above City Creek; terrace appears to grade to the Provo level shoreline; exposed thickness less than 15 feet (5 m).

Qafy **Younger alluvial-fan deposits, undivided** (Holocene to Late Pleistocene?) – Poorly to moderately sorted, pebble to cobble gravel with boulders near bedrock sources, grading to mixtures of sand, silt, and clay on gentler slopes; matrix is sand, silt, and clay; clasts angular to subrounded; deposited by debris flows, debris floods, and streams at the mouths of canyons throughout the quadrangle; includes both ages of younger alluvial-fan deposits; postdates the regression of Lake Bonneville from the Provo shoreline and lower shorelines; a more specific age cannot be determined where not incised by active streams, or where areas of Qaf_1 and Qaf_2 are too small to show separately at map scale; thickness variable, most deposits between about 10 and 40 feet (3–12 m) thick, but could be locally thicker.

Qafp **Alluvial-fan deposits, related to Provo shoreline and regressive phase of Lake Bonneville** (Late Pleistocene) – Poorly to moderately sorted, pebble to cobble gravel, locally bouldery, in a matrix of sand, silt, and minor clay; clasts typically angular but well-rounded where derived from Lake Bonneville gravel; deposited by debris flows, debris floods, and streams; mapped along North Canyon where the upper surface of the alluvial fan is graded to the Provo shoreline; deposited during the overflowing phase of the lake; incised by younger alluvial deposits (Qal_1); exposed thickness less than 30 feet (9 m).

Qafb **Alluvial-fan deposits, related to Bonneville shoreline and transgressive phase of Lake Bonneville** (Late Pleistocene) – Poorly to moderately sorted, pebble to cobble gravel, locally bouldery, with a matrix of sand, silt, and minor clay; clasts angular to subangular but well-rounded where derived from Lake Bonneville gravel; deposited by debris flows, debris floods, and streams; mapped immediately above, and are graded to, the Bonneville shoreline on the north side of the Salt Lake salient; exposed thickness less than 15 feet (5 m).

Colluvial Deposits

Qc **Colluvial deposits** (Holocene to Middle Pleistocene?) – Poorly to moderately sorted, generally poorly stratified, clay- to boulder-size, locally derived sediment; deposited by slope wash and soil creep on steep slopes; may include landslides, rockfalls, debris flows, and alluvial-fan deposits that are too small to map separately; most bedrock is covered by at least a thin veneer of colluvium, but only the larger, thicker (> 3 feet [1 m]) deposits are mapped; thickness less than 15 feet (5 m).

Human-Derived

Qh **Fill and disturbed land** (historical) – Undifferentiated fill and disturbed land related to the construction of canals, landfills, road embankments, water control structures used for wetlands mitigation, migratory bird refuges, duck club ponds, Interstates 80, 15, and 215, and railroad lines; only the larger areas of disturbed land are mapped; unmapped fill and disturbed lands are present in most developed areas and contain continually changing mix of cuts and fills; thickness highly variable, interstate and rail embankments up to about 50 feet (~16 m).

Qhr **Remediated land** (historical) – Unit delineates approximate boundaries of selected environmentally remediated sites in the quadrangle, Portland Cement kiln dust #2 and #3, and Rose Park sludge pit, both described below; other remediated lands may exist in the quadrangle and, where mapped, the extent of surficial (soil) or groundwater contamination may exceed the unit boundaries; areas near remediated sites may contain latent contaminated material or groundwater and a comprehensive site-specific environmental investigation is recommended prior to development; thickness of remediated material is variable to unknown.

Portland Cement kiln dust sites #2 and #3 are a combined remediation zone within an approximately 71-acre triangular area west of Redwood Road (at about 1000 S. Redwood Road) between Indiana Avenue and the Jordan River Surplus Canal (section 10, T. 1 S., R. 1 W.). The full remediated site described here includes a large area in the adjacent Salt Lake City South quadrangle (McKean, 2019b). Between 1965 and 1983, cement kiln dust and chromium-bearing refractory kiln bricks were disposed at the site (U.S. Environmental Protection Agency [EPA], 1992). The dust and bricks were waste from a cement plant located at the southwest corner of 600 West Street and 800 South Street that was operated by several companies. Site remediation took place between 1995 and 1998, during which the waste was removed, treated, and disposed off-site (EPA, undated). Groundwater monitoring is ongoing (EPA, undated). The site is now being developed and is partially occupied by several warehouses.

The Rose Park sludge-pit site is located on the north side of Rosewood Park in Salt Lake City (section 23, T. 1 N., R. 1 W.). The following information is a summary of the site history from Fred C. Hart Associates, Inc. (1980) and Smidinger (2017). The 5.5-acre site was used by Utah Oil and Refining Company (later a subsidiary of Amoco Oil Company) to dispose of refinery waste from the 1930s until 1955. In 1957, Salt Lake City purchased the site and in 1960, removed 100 truckloads of the sludge and covered the pit with a soil cap. Development of the park in 1976 exposed residual waste from the original pit. Site investigation took place from 1979 to 1983. Remediation conducted between 1983 and 1992 included a bentonite slurry wall around the perimeter, an engineered cap constructed over the waste material, and signage and barriers restricting access to the site. Groundwater monitoring and site inspections continue at the site (Smidinger, 2017).

Lacustrine and Deltaic Deposits

Deposits related to Great Salt Lake: Located at and below Great Salt Lake Early Holocene highstand shoreline elevation of about 4230 feet (1289 m) in the Salt Lake City North quadrangle (Table 1).

Qdy **Young deltaic deposits** (Late to Middle? Holocene) – Poorly to moderately sorted, yellowish-gray to yellowish-brown sand, silt, and minor clay; sand is very fine to medium grained and subangular to angular; sand grains are quartz, lithic fragments, and mica flakes; thin to medium bedded; located along the west side of the Jordan River at the end of paleo-Jordan River distributary channels (section 17, T. 1 N., R. 1 W. and section 31, T. 2 N., R. 1 W.); mapped where distinct delta lobes overlie lacustrine sediments; locally includes a surficial loess veneer; exposed thickness less than 6 feet (2 m).

Qdd, Qdd?

Deltaic distributary channel deposits (Late to Middle? Holocene) – Moderately sorted, yellowish-gray to light olive-gray silt with sand and clay; includes natural levee deposits; sand is very fine to fine grained; contains thin discontinuous sand lenses; subangular to angular sand grains; thin to medium bedded; sand grains include quartz, lithic fragments, and mica flakes; located in northwest quadrant of map where delta distributary channels incised down through the young lacustrine and deltaic deposits (Qldy) and deposited fluvial sediments and associated natural levee deposits over Qldy; based on elevation, the delta deposits appeared to have entered the Late Holocene highstand of Great Salt Lake and also represent the northeastward migration of the Jordan River from a previous Holocene delta system that had dominantly northwest-directed channels (Murchison, 1989; McKean and Hylland, 2019a, 2019b); locally includes a loess veneer and buried soil; exposed thickness less than 10 feet (3 m).

Qlos **Lacustrine oolitic sand deposits** (Holocene) – Moderately to well-sorted, light olive-gray to yellowish-gray oolitic sand, carbonate chips and clasts, and minor silt; oolitic sand is medium to coarse grained; quartz and lithic sand grains are angular to subangular and ooid sand grains are rounded to subrounded; carbonate chips and clasts are subrounded to angular; thin to medium bedded; sand grains vary from 10% to 75% ooids (with higher concentrations near the Great Salt Lake beach ridge crest in the adjacent Baileys Lake quadrangle, McKean and Hylland, 2019a), with varying amounts of quartz, lithic fragments, carbonate fragments, and mica flakes; carbonate chips and clasts are 0.5 to 6 inches (1–15 cm) in diameter and 1 to 2 inches (3–5 cm) thick; ooids formed in Great Salt Lake and were deposited on delta barrier bars and islands by wave action; carbonate chips and clasts, commonly flat in shape, appear to be rip-up clasts of cemented ooids and/or laminated algal mats or microbialite carbonates that washed up on shore; mapped in one location in the northwest corner of the quadrangle on a small island near the average 4200 foot elevation Great Salt Lake shoreline; mapped on elevated surfaces above young lacustrine mud deposits (Qlmy), typically overlies lacustrine silt and clay deposits; thickness 1 to 6 feet (0.3–2 m).

Deposits of Great Salt Lake, Gilbert-episode lake, and Lake Bonneville: Mapped below the Bonneville highstand shoreline. The Bonneville shoreline is at elevations of about 5180 to 5200 feet (1579–1585 m) in the Salt Lake City North quadrangle (Table 1).

Qldy **Young lacustrine and deltaic deposits** (Holocene to Late Pleistocene) – Well to moderately sorted, light olive-gray to moderate yellowish-brown, silty sand and clay; commonly more clay rich with very little silt and sand; thin to medium bedded; sand is fine to medium grained with subangular to rounded grains of quartz, lithics, and mica; located in the western part of the map; distinguished from deltaic deposits (Qdy) by its broad uniformly flat geomorphic surface along the paleo-Jordan River channels and deltas; distinguished from young lacustrine deposits (Qly) because it is overlain and incised by alluvial channels (Qaly), deltaic distributary channels (Qdd), and deltaic deposits (Qdy); locally includes a surficial loess veneer and a buried soil; exposed in a paleoseismic trench in the adjacent Baileys Lake quadrangle investigated by Hylland et al. (2014), where this unit was underlain by a tufa-breccia and clay related to the Gilbert-episode lake, as well as Lake Bonneville olive-gray and red-brown clays and olive-gray quartz sands (Hylland et al., 2014), unit may include clay related to Gilbert-episode lake or regressive phase of Lake Bonneville; loess in this unit probably correlates with the loess (unit Qldy) at the Baileys Lake paleoseismic trench site (Hylland et al., 2014; McKean and Hylland, 2019a); exposed thickness less than 10 feet (3 m).

Qlmy **Young lacustrine mud deposits** (Holocene to Late Pleistocene?) – Moderately to well-sorted, yellowish-brown to olive-gray silt, clay, and minor sand; sand is fine to medium grained; silt is unbedded with thin discontinuous stringers of clay and sand; clay is light olive-gray to olive-gray marl and is locally mottled; the sand is olive gray to moderate brown and composed of subangular to angular grains of quartz, lithic fragments, and mica flakes, and locally ooids; locally includes halite, gypsum, and other salts that form thin deposits on the ground surface; mapped in northwest part of the quadrangle between lacustrine and deltaic sediments (Qly, Qldy) on lightly to non-vegetated mud flats that are flooded periodically by Great Salt Lake, shallow groundwater, or occasionally by water-control structures that flood these lowlands for wetlands mitigation or ponding for duck hunting clubs and bird refuges; distinguished on aerial photographs from Qly by the characteristic, low-lying, white mud flats and lack of vegetation; includes mud flats from Holocene highstands above the historical highstand of Great Salt Lake; in places, the unit forms a thin veneer over the underlying Gilbert-age tufa breccia (tufa found in the subsurface as a cemented layer or broken pebble-size clasts) and clay, and Lake Bonneville-age olive-gray and red-brown clay and olive-gray quartz sands (see Figure 4 McKean and Hylland, 2019a) (Hylland et al., 2012, 2014); unit may include Gilbert or regressive Bonneville clays where the Gilbert tufa is absent; estimated less than 10 feet (3 m) thick.

Qly **Young lacustrine deposits** (Holocene to Late Pleistocene?) – Moderately sorted silt, sand, clay, and marl; dark yellowish-brown silt, olive-gray quartz sand, light olive-gray clay, and yellowish-gray marl; quartz sand is fine to coarse grained and subangular to angular; sand locally contains ooids (5% to 15%); mapped in west part of quadrangle where lacustrine sediments form low "islands" or elevated mounds, surrounded by or including young lacustrine mud deposits (Qlmy) and spring and marsh deposits (Qsm); distinguished from Qlmy by the presence of vegetation, the lack of mud flats, and an elevated island-like geomorphology; distinguished from younger deltaic (Qdy) and lacustrine and deltaic (Qldy) deposits by the lack of natural levee deposits and deltaic distributary channels; as mapped, unit may include or be underlain by Gilbert-age tufa breccia (tufa found in the subsurface as a cemented layer or broken pebble-size clasts) and clays, and Lake Bonneville-age olive-gray and red-brown clays and olive-gray quartz sands (Hylland et al., 2012, 2014); deposits have erosional and depositional Great Salt Lake shorelines on them; locally includes a loess veneer and buried soil; includes deposits from three historical lakes mentioned on Van Horn's surficial geologic map (1982): Hot Springs Lake (1869 and 1934) at Becks Hot Springs (sections 10, 11, 14, 15, and 23, T. 1 N., R. 1 W.), Williams Lake (1906) (sections 31 and 32, T. 1 N., R. 1 W. and section 6 T. 1 S., R. 1 W.), and Smith Lake (1906) (section 4, T. 1 S., R. 1 W.), which appear to have formed in depressions potentially related to faulting on the Warm Springs, Taylorsville, and Granger faults, respectively (McKean and Hylland, 2019b); G.K. Gilbert in 1890 suggested that the Hot Springs Lake represented an area of local subsidence related to the Warm Springs fault that had not been filled in by the Jordan River (in Hunt, 1982, p. 27), but the lake could have also formed behind a natural levee of the Jordan River (Scott and Shroba, 1985); exposed thickness less than 6 feet (2 m).

Qlf **Lacustrine fine-grained deposits** (Holocene to Late Pleistocene) – Interbedded deposits of moderately to well-sorted sand, silt, and minor clay; angular to rounded sand; locally may contain areas of more silt and clay with minor sands; typically thin bedded; mapped in the east part of the quadrangle; deposits include those of Lake Bonneville transgression and regression, the Gilbert-episode inundation, and the undivided Holocene highstands of Great Salt Lake; interbedded or laterally gradational with areas of lacustrine gravel and sand and young alluvial deposits (Qlgp and Qaly, respectively); age correlative to lacustrine and deltaic units in west part of map area; estimated thickness 15 feet (5 m).

Deposits related to Lake Bonneville: Mapped below the Bonneville shoreline. The Bonneville shoreline is at elevations of about 5180 to 5200 feet (1579–1585 m) but above the Gilbert shoreline in the Salt Lake City North quadrangle (Table 1).

Ql **Lake Bonneville and pre-Bonneville deposits, undivided** (Late Pleistocene) – Moderately to well-sorted deposits of subrounded to rounded, fine to coarse sand, silt, and clay with pebbly gravel; limited to exposures in bluffs along the east side of City Creek Canyon where slope colluvium conceals the relative amounts of sand, silt, and clay in these deposits; may include alluvial, deltaic, and pre-Bonneville deposits that cannot be differentiated; exposed thickness less than 180 feet (55 m).

Deposits related to the Provo shoreline and regressive phase of Lake Bonneville: Located at and below the Provo shoreline elevation, about 4820 to 4860 feet (1469–1482 m) but above the Gilbert-episode shoreline elevation in the Salt Lake City North quadrangle (Table 1).

Qdp **Deltaic deposits** (Late Pleistocene) – Moderately to well-sorted, pebble and cobble gravel with a matrix of sand and silt; deposited as thin to thick planar and foreset beds; locally includes topset beds and thin beds of silt and sandy silt; clasts subrounded to rounded; mapped at the mouth of City Creek Canyon where the delta related to the Provo shoreline and Lake Bonneville regression is incised by the younger City Creek; exposed thickness less than 120 feet (35 m).

Qlgp **Lacustrine gravel and sand** (Late Pleistocene) – Moderately to well-sorted, pebble- to cobble-gravel with a matrix of sand, silt, and clay; clasts commonly subrounded to rounded, but some deposits consist of poorly sorted, angular gravel derived from nearby bedrock outcrops; gravel locally cemented with calcium carbonate; local tufa deposits northeast of Victory Road (SE¼ section 25, T. 1 N., R. 1 W.), mapped as part of stacked unit Qlgp/Tcl; thin to thick bedded; locally interbedded with thin to thick beds of silt and pebbly sand; locally deposits are veneers over bedrock; typically deposited below wave-cut benches close to the Provo shoreline around the perimeter of the Salt Lake salient; thickness likely greater than 50 feet (15 m).

Deposits related to the Bonneville shoreline and transgressive phase of Lake Bonneville: Mapped between the Bonneville shoreline and Provo shoreline. The Bonneville shoreline is at elevations from about 5180 to 5200 feet (1579–1585 m) in the Salt Lake City North quadrangle (Table 1).

Qldgb **Lacustrine and deltaic gravel and sand** (Late Pleistocene) – Moderately to well-sorted gravel and sand, locally includes thin beds of silt and sandy silt; clasts subrounded to rounded; thin to thick, planar- and cross-bedded foreset beds; locally includes topset alluvial beds; locally weakly cemented with calcium carbonate; mapped east of the mouth of City Creek Canyon where deltaic deposits were likely reworked and pushed southeast by longshore currents; estimated thickness less than 130 feet (40 m).

Qlgb **Lacustrine gravel and sand** (Late Pleistocene) – Moderately to well-sorted, pebble- to cobble-gravel with a matrix of sand and silt; clasts commonly subrounded to rounded, but some deposits consist of poorly sorted, angular gravel derived from nearby bedrock outcrops; gravel locally cemented with calcium carbonate; thin to thick bedded; locally interbedded with thin to thick beds of silt and pebbly sand; locally deposits are veneers over bedrock; deposited at or below the Bonneville shoreline; thickness likely greater than 50 feet (15 m).

Mass-Movement Deposits

Qml **Lateral spread deposits** (Holocene to Late Pleistocene?) – Poorly sorted clay- to boulder-size blocks of material in displaced sediment, with grain size varying with the nature of source material; deposited by liquefaction-induced landslides triggered by strong earthquake ground motion; characterized by displaced sediment in slumps and rotated blocks, chaotic bedding, small grabens with little to no offset that sole into the basal detachment of the landslide, hummocky topography, and main and internal scarps; thickness highly variable.

Three deposits are present in the quadrangle, in section 6, T. 1 S., R. 1 E. and section 1 T. 1 S., R. 1 W. (1) Excavations for the former Hall of Justice building, near 500 South and 300 East Streets, revealed numerous high-angle faults and other deformation features that are likely lateral-spread deposits and not related to tectonic faults (Osmond et al., 1965; Scott and Shroba, 1985). (2) Scott and Shroba (1985) discuss a lateral spread deposit mapped by Van Horn (1982), between South Temple and 300 South and between 200 East and 600 East in Salt Lake City, that was inferred from numerous faults and other evidence of deformation in Lake Bonneville and older deposits. (3) At the Salt Palace Convention Center expansion project (near 200 South and between 200 West and West Temple), grabens were discovered within the construction footprint by consultants' geotechnical investigations (Kleinfelder, Inc., 1999; Simon Bymaster, Inc., 1999). The two investigations gave conflicting reports of possible tectonic faulting, liquefaction-induced lateral spreading, or some combination of the two processes (see Geologic Hazards section for more information). Seismic surveys by Liberty et al. (2021) identified faulting and lateral spreading at the former Hall of Justice and the Salt Palace Convention Center locations and discussed evidence for other potential lateral spread deposits in the area. Their data shows that more lateral spread deposits likely exist in the quadrangle, but urbanization has concealed evidence of the deposits (see Figure 2 in Liberty et al., 2021). Age and stability determinations require detailed geotechnical investigations.

Qml_3 **North Salt Lake lateral spread deposit** (Early Holocene? to Late Pleistocene?) – Poorly sorted clay- to boulder-size blocks of material in displaced sediment, with grain size varying with the nature of source material; deposited by liquefaction-induced landslides triggered by strong earthquake ground motion; characterized by displaced sediment in slumps and rotated blocks, chaotic bedding, small grabens with little to no offset that sole into the basal detachment of the landslide, hummocky topography, and main and internal scarps; identification and extent based on: 1) hummocky topography visible on 1937 USDA aerial photographs; 2) previous mapping (Van Horn, 1982; Harty and Lowe, 2003); 3) multiple accounts of contorted bedding, shallow listric faults, and other deformation (Robison et al., 1991; Anderson et al., 1994; Harty and Lowe, 2003), and 4) a continuous, undeformed bed beneath the lateral spread (Robison et al., 1991); originally mapped by Van Horn (1982) as two distinct slides, an older one to the south and a younger one to the north; we also map two slide masses, based on cross-cutting relationships with the younger one to the north, but suggest both their ages are relatively similar and have not given them separate age designations; age of both slides is constrained by the Bonneville-age (Late Pleistocene) lacustrine sediments which are the parent material for the slides and possible Gilbert-episode shoreline (Early Holocene to Early Pleistocene?) that is developed on the lateral spread deposits (Robison et al., 1991); age and stability determinations require detailed geotechnical investigations; thickness highly variable.

Qmsh **Historical landslide deposits** (historical to Late Pleistocene?) – Poorly sorted clay- to boulder-size material, grain size dependent on source material; deposited by slides, slumps, and earth flows; characterized by hummocky topography, main and internal scarps, toe thrusts, back-rotated blocks, and chaotic bedding in displaced bedrock; nine landslides identified as having historical movement (including the Springhill, Parkway Drive, and City Creek landslides, see Landslide subsection for more details on the location and movement history of these landslides); historical age based on written or verbal accounts of movement, observations during mapping, or where movement is detectible between different ages of aerial photographs ranging from 1977, mid-1990s, and 2011 (UGRC, 1977, mid-1990s, 2011a); even landslides with subdued morphology (suggesting that they are older, weathered, and have not moved recently) may continue to exhibit slow creep or are capable of renewed movement if stability thresholds are exceeded (Ashland, 2003); age and stability determinations require detailed geotechnical investigations; many small or thin landslides maybe present throughout the quadrangle but not mapped due to map scale limitations; thickness highly variable.

Qms **Landslide deposits** (historical? to Middle Pleistocene?) – Poorly sorted clay- to boulder-size material, grain size dependent on source material; deposited by slides, slumps, and earth flows; characterized by hummocky topography, main and internal scarps, toe thrusts, back-rotated blocks, and chaotic bedding in displaced bedrock; mapped mainly above the Bonneville shoreline on the Salt Lake salient; not subdivided by apparent age because even landslides with subdued morphology (suggesting that they are older, weathered, and have not moved recently) may continue to exhibit slow creep or are capable of renewed movement if stability thresholds are exceeded (Ashland, 2003); age and stability determinations require detailed geotechnical investigations; many smaller landslides maybe present throughout the quadrangle but not mapped because they are too small to show at map scale; thickness highly variable.

Qmt **Talus deposits** (historical to Middle Pleistocene?) – Poorly sorted pebble- to boulder-size, locally derived material; clasts subangular to angular; ranges from fresh, active rockfall deposits to partially vegetated and stabilized slopes; large boulders visible in aerial photographs of the deposit that suggest a prolonged history of rockfall in the area; only one deposit mapped north of Oak Forest Road in Salt Lake City (SE1/4, section 19, T. 1 N., R. 1 E.), within which a historical rockfall event occurred on April 17 or 18, 1999 (Rich Giraud, UGS, verbal communication, 2013, see Rockfall subsection); fractures are visible in the overlying cliffs that are composed of Paleogene upper conglomerate (Tcu) bedrock, future rockfall may occur in the immediate area; stability determinations and mitigation recommendations require detailed geotechnical investigations; small and thin talus deposits are present on numerous slopes but not mapped due to map scale; estimated thickness 0 to 30 feet (0–10 m).

Spring and Marsh Deposits

Qsm **Spring and marsh deposits** (Holocene to Late Pleistocene?) – Silt, clay, and organic-rich sediment associated with springs, ponds, seeps, and wetlands; may locally contain peat deposits; commonly wet, but seasonally dry; overlies young lacustrine deposits (Qly); distinguished from young lacustrine mud deposits (Qlmy) by the presence of wetlands and the lack of salt crust and alluvial meanders, deltaic lobes, and/or lacustrine mud flat deposits on aerial imagery; mapped in northwest part of the quadrangle where the water table is high and ponds support the growth of tall reeds, which is a distinguishing feature on aerial photographs; some marsh deposits may be the result of impounded water and wetlands controlled by dikes and water-control actions of the duck hunting clubs and migratory bird refuges; small spring and marsh deposits are present in the quadrangle but are not mappable due to scale limitations; estimated thickness less than 6 feet (2 m).

Mixed-Environment Deposits

Qalh **Historical alluvial deposits and artificial levees, undivided** (historical) – Mainly modified channel margins and engineered levees along the active channel of the Jordan River, which has been largely modified from its natural stream course and channelized; locally includes minor natural terraces less than 10 feet (3 m) above the active channel that are medium bedded, moderately sorted sand, silt, and minor clay deposits; locally includes minor colluvial deposits along steep stream embankments; exposed thickness less than 25 feet (8 m).

Qac **Alluvial and colluvial deposits, undivided** (Holocene to Middle Pleistocene?) – Poorly to moderately sorted, generally poorly stratified, clay- to boulder-size, locally derived sediment; rounded to angular clasts; aggraded deposits in bottoms of drainages and on adjacent slopes; deposited by slopewash, soil creep, floods, and minor perennial fluvial processes on the Salt Lake salient; includes debris-flows, talus, stream deposits, alluvial-terrace deposits, earth-flow deposits, small fans, and minor landslides that are too small to map separately; incised 0 to 12 feet (0–4 m) by modern drainages; channels that these deposits occupy have potential for debris flows and floods; thickness less than 60 feet (20 m).

Qad **Alluvial-fan and Lake Bonneville deltaic deposits, undivided** (Holocene to Late Pleistocene) – Poorly to well sorted clay, silt, sand, gravel, cobbles, and boulders; clasts rounded to angular; thin to medium bedded; locally gravel-poor and clay and silt rich; mapped west of City Creek Canyon where local alluvial fans interfinger and overlie mixed lacustrine and alluvial-deltaic deposits of Lake Bonneville; exposed thickness approximately 15 to 30 feet (5–10 m).

Qam **Alluvial and marsh deposits** (Holocene) – Moderately to well-sorted sand, silt, clay, and organic-rich sediment associated with springs, ponds, seeps, wetlands and alluvial channels and oxbow lakes of the Holocene Jordan River flood plain; locally contains peat deposits; mapped north of Interstate 215 along the Jordan River (north of section 4, T. 1 N., R. 1 W.); commonly wet, but seasonally dry; associated with a high water table and ponds that support the growth of tall reeds, which aid in distinguishing these deposits on aerial photographs; distinguished from unit Qsm (spring and marsh deposits) by association with oxbow lakes of the Jordan River; estimated thickness less than 15 feet (5 m).

Qla **Lacustrine and alluvial deposits, undivided** (Holocene to Middle Pleistocene) – Gravel, sand, silt, and clay; lacustrine deposits typically finer grained (silt and clay dominated) and interbedded with coarser-grained (sand and silt dominated) alluvial deposits; locally includes a component of loess; mapped where alluvial and lacustrine deposits grade imperceptibly into one another; mapped adjacent to alluvial fans along the Warm Springs fault and on terraces 5 to 20 feet (1.5–7 m) above the Jordan River; estimated thickness 15 feet (5 m).

Qlam **Lacustrine, alluvial, and marsh deposits, undivided** (Holocene to Late Pleistocene) – Silt, clay, and minor sand and pebbles; organic-rich sediment associated with springs, ponds, seeps, and other wetlands; commonly wet, but seasonally dry; mapped in areas where marsh, alluvial, and lacustrine deposits may be patchy and intermixed, and cannot be shown separately at map scale; estimated thickness 15 feet (5 m).

Qmc **Landslide and colluvium deposits, undivided** (Holocene to Late Pleistocene?) – Poorly sorted to unsorted clay- to boulder-size material; mixed landslide, slump, slopewash, and soil creep that are gradational imperceptibly into one another; typically have a hummocky appearance on the slope-shade images derived from lidar but lack clear landslide scarps and flanks; mapped where cannot show colluvium separately from landslides at map scale and along City Creek Canyon where eroded hummocky Lake Bonneville deposits are slumping into the creek; thickness 0 to more than 30 feet (0–10+ m).

Stacked-Unit Deposits

The term "stacked" means a thin covering of one unit over the other, which is shown by the upper map unit (listed first), followed by a slash, then the underlying unit. See individual map unit descriptions for more information regarding materials.

Qafy/Qml$_3$

Younger alluvial-fan deposits, undivided over North Salt Lake lateral spread deposit (Holocene to Late Pleistocene/Early Holocene? to Late Pleistocene?) – A veneer of younger alluvial-fan deposits over older lateral spread deposits; alluvial-fan deposits are likely less than 10 feet (3 m) thick and the estimated thickness of lateral spread deposits are highly variable.

Qafy/Qml

Younger alluvial-fan deposits, undivided over lateral spread deposits (Holocene to Late Pleistocene/Holocene to Middle Pleistocene) – A veneer of younger alluvial-fan deposits over lateral spread deposits; alluvial-fan deposits are likely less than 10 feet (3 m) thick, and the estimated thickness of lateral spread deposits are highly variable.

Qc/Tcu

Qc/Tt **Colluvial deposits over Paleogene bedrock** (Holocene to Middle Pleistocene/Miocene? to Eocene) – A veneer of colluvium and soil development has concealed the upper conglomerate (Tcu) and tuffaceous strata (Tt); however, in erosional gullies and road cuts the Paleogene units are identifiable; cobbles and boulders in the colluvium float represent the upper conglomerate (Tcu), whereas the tuffaceous strata are slope forming; mapped on the Salt Lake salient near Hell Canyon; colluvial material has variable thickness between 0 and 10 feet (0–3 m).

Qh/Qaly

Fill and disturbed land over young stream deposits, undivided (historical/Holocene) – Undifferentiated earth fill and disturbed land associated with the Salt Lake City International Airport concealing young stream deposits associated with the paleo-Jordan River channel that flowed northwest towards Great Salt Lake (McKean and Hylland, 2019a, 2019b); pre-development geology interpreted from 1937 USDA aerial photographs; thickness of fill and disturbed land highly variable, stream deposits estimated thickness less than 15 feet (5 m).

Qh/Qafy

Fill and disturbed land over younger alluvial-fan deposits (historical/ Holocene to Late Pleistocene) – Undifferentiated earth fill and disturbed land along Interstate 15, conceal younger alluvial-fan deposits; pre-development geology interpreted from 1937 USDA aerial photographs; thickness of fill and disturbed land and alluvial-fan deposits are highly variable.

Qh/Qly **Fill and disturbed land over young lacustrine deposits of Great Salt Lake, Gilbert-episode lake, and Lake Bonneville** (historical/Holocene to Late Pleistocene) – Undifferentiated earth fill and disturbed land associated with the Salt Lake City International Airport and a refinery near Interstates 15 and 215 interchange; pre-development geology interpreted from 1937 USDA aerial photographs; thickness of fill and disturbed land highly variable, lacustrine deposits estimated thickness 15 feet (5 m).

Qh/Qlf **Fill and disturbed land over lacustrine fine-grained undivided deposits of Lake Bonneville, Gilbert-episode lake, and Great Salt Lake** (historical/Holocene to Late Pleistocene) – Undifferentiated earth fill and disturbed land associated with the refinery near Interstates 15 and 215 interchange; pre-development geology interpreted from 1937 USDA aerial photographs; thickness of fill and disturbed land highly variable, lacustrine deposits estimated thickness 15 feet (5 m).

Qh/Qldy

Fill and disturbed land over young lacustrine and deltaic deposits of Lake Bonneville, Gilbert-episode lake, and Great Salt Lake (historical/Holocene to Late Pleistocene) – Undifferentiated earth fill and disturbed land associated with the Salt Lake City International Airport concealing lacustrine and deltaic deposits; pre-development geology interpreted from 1937 USDA aerial photographs; thickness of fill and disturbed land highly variable, exposed lacustrine and deltaic thickness less than 10 feet (3 m).

Qh/Qla **Fill and disturbed land over lacustrine and alluvial deposits, undivided** (historical/Holocene to Middle Pleistocene) – Undifferentiated earth fill and disturbed land associated with the Salt Lake City International Airport concealing lacustrine and alluvial deposits along the southeastern part of the airport; pre-development geology interpreted from 1937 USDA aerial photographs; thickness of fill and disturbed land highly variable, lacustrine and alluvial deposits estimated thickness less than 15 feet (5 m).

Qh/Qlam

Fill and disturbed land over lacustrine, alluvial, and marsh deposits, undivided (historical/ Holocene to Late Pleistocene) – Undifferentiated earth fill and disturbed land associated with the refinery and Interstate 15; pre-development geology interpreted from 1937 USDA aerial photographs; thickness of fill and disturbed land highly variable, marsh, alluvial, and lacustrine deposits estimated thickness 15 feet (5 m).

Qlgp/Tv

Qlgp/Tt

Qlgp/Tcl

Lacustrine gravel and sand related to the Provo shoreline and regressive phase of Lake Bonneville over Paleogene bedrock (Late Pleistocene/Eocene to Paleocene?) – A veneer of lacustrine gravel and sand, related to the overflowing and regressive phases of Lake Bonneville, partially concealing Paleogene bedrock (Tv, Tt, and Tcl); mapped on the west part of the Salt Lake salient where bedrock knobs are exposed intermittently within the lacustrine units but unable to map separately due to map scale; stacked unit Qlgp/Tcl contains local tufa deposits northeast of Victory Road (SE¼ section 25, T. 1 N., R. 1 W.); lacustrine gravel and sand thickness likely between 3 and 50 feet (1–15 m), for Paleogene bedrock thicknesses see individual unit descriptions.

Qlgp/Mdo

Qlgp/Mdo?

Qlgp/Mh

Qlgp/Md

Qlgp/Mg

Qlgp/Dpp

Qlgp/Dst

Qlgp/Єu

Lacustrine gravel and sand related to the Provo shoreline and regressive phase of Lake Bonneville over Paleozoic bedrock (Late Pleistocene/Late Mississippian to Middle Cambrian) – A veneer of lacustrine gravel and sand, related to the overflowing and regressive phases of Lake Bonneville, over Paleozoic bedrock units (Mdo, Mh, Md, Mg, Dpp, Dst, and Єu); mapped on the west part of the Salt Lake salient; bedrock knobs are included in the unit and not mapped separately due to map scale limitations; lacustrine gravel and sand thickness likely between 3 and 50 feet (1–15 m), for Paleozoic bedrock thicknesses see individual unit descriptions.

Qldgb/Tcu

Deltaic deposits related to the Bonneville shoreline and transgressive phase of Lake Bonneville over upper conglomerate (Late Pleistocene/Miocene? to Oligocene?) – A veneer of lacustrine and deltaic gravel and sand, related to the transgressive phase of Lake Bonneville, concealing lower conglomerate; mapped on the west part of the Salt Lake salient near City Creek Canyon where bedrock knobs are exposed intermittently within the lacustrine units but unable to map separately due to map scale lacustrine gravel and sand thickness likely between 3 and 50 feet (1–15 m), for Paleogene bedrock (Tcu) estimated unit thickness in the quadrangle 500 to 1600 feet (150–500 m).

Qlgb/Tt

Qlgb/Tcl

Lacustrine gravel and sand related to the Bonneville shoreline and transgressive phase of Lake Bonneville over Paleogene bedrock (Late Pleistocene/Eocene to Paleocene?) – A veneer of lacustrine gravel and sand, related to the transgressive phase of Lake Bonneville, concealing Paleogene bedrock (Tt and Tcl); mapped on the west part of the Salt Lake salient where bedrock knobs are exposed intermittently within the lacustrine units but unable to map separately due to map scale; lacustrine gravel and sand thickness likely between 3 and 50 feet (1–15 m), for Paleogene bedrock thicknesses see individual unit descriptions.

Qlgb/Mdo

Qlgb/Mh

Qlgb/Md

Qlgb/Єu

Lacustrine gravel and sand related to the Bonneville shoreline and transgressive phase of Lake Bonneville over Paleozoic bedrock (Late Pleistocene/Late Mississippian to Middle Cambrian) – A veneer of lacustrine gravel and sand, related to the transgressive phase of Lake Bonneville, over Paleozoic bedrock units (Mdo, Mh, Md, and Єu);

mapped on the west part of the Salt Lake salient where bedrock knobs are exposed intermittently within the lacustrine units but unable to map separately due to map scale lacustrine gravel and sand thickness likely between 3 and 50 feet (1–15 m), for Paleozoic bedrock thicknesses see individual unit descriptions.

Unconformity

QUATERNARY/NEOGENE (TERTIARY)

QTa **Old alluvial deposits** (Early Pleistocene? to Pliocene?) – Unconsolidated gravel and sand that is locally semi-consolidated, composed of sand, pebble-, cobble- and boulder-size clasts; clasts are subrounded to subangular, composed of dominantly sandstone and quartzite with minor limestone and older conglomerate (Tcl and Tcu); forms a flat, cobble-armored surface that caps the west part of the Salt Lake salient and is easily identifiable in stereo-photography and lidar-derived images; flat, armored surface is commonly underlain by a colluvium-covered slope, could be semi-consolidated to unconsolidated; lower contact is unconformable with Tcu and, in places difficult to distinguish from Tcu; Van Horn (1981) mapped this unit as the late Tertiary Hooper Canyon Formation of late Tertiary age; potentially caps many ridges of the Salt Lake salient but poor exposure, similarity of clast composition to Tcu, and lack of distinct geomorphic surfaces has precluded distinction; likely deposited only in the hanging wall of the Rudys Flat fault, potentially before activation of the Warm Springs fault and uplift of the Salt Lake salient (see Anderson and McKean, 2018); uncertain age range, possibly Early Pleistocene or Pliocene based on stratigraphic position and footwall uplift rates of the Wasatch fault zone (Anderson and McKean, 2018); estimated thickness 20 to 60 feet (6–18 m).

Unconformity

NEOGENE TO PALEOGENE (TERTIARY)

Tcu **Upper conglomerate** (Miocene? to Eocene?) – Light-brown to brownish-orange, moderate to well-cemented, conglomerate composed of pebble-, cobble- and boulder-size clasts; contains thin, discontinuous sandstone lenses composed of fine- to medium-grained quartz and lithic sand with a calcium carbonate cement; conglomerate is clast- and matrix-supported with a sandy matrix; rounded to subangular clasts mainly composed of Paleozoic limestone, tan sandstone, light-red sandstone, quartzite, and older conglomerate (Tcl); metamorphic clasts of locally derived, Paleoproterozoic Farmington Canyon Complex are more common on the north side of the Salt Lake salient; largest clast about 3 feet (~1 m); no volcanic clasts observed; forms cliffs and steep to moderate slopes; most of the unit is poorly exposed and covered by a thin to thick layer of colluvium or other Quaternary deposits; the base of the unit is difficult to distinguish in the field due to poor exposures, but is generally mapped at or near the appearance of conglomerate beds (or float) that contain clasts of older conglomerate (Tcl) and where float of unit Tt disappears when walking upslope; lower contact is unconformable with units Tt, Tv, and Tcl and is commonly angularly discordant; Mann (1974) measured paleoflow directions from imbricated clasts and determined a southeast-to-northwest paleocurrent direction for the deposit—the western flow direction and lack of young zircons suggest that a major component of the unit's source area was the Wasatch Range directly to the north and east of the Rudys Flat fault; a U-Pb detrital zircon sample (SLCN2014-287) from a sand lens in this unit contained no grains younger than the Triassic (McKean et al., 2016), detrital zircon U-Pb age data for the Fort Douglas quadrangle to the east show that Tcu contains sparse Cenozoic zircons, that potentially indicate a maximum depositional age of Early Oligocene (Anderson and McKean, 2018; Anderson et al., 2024); dips up to ~30° and the lack of Miocene zircon grains in Tcu, which would suggest time-equivalence to the tephra-rich Middle Miocene to Early Pliocene Salt Lake Formation in the surrounding area (Oaks et al., 1999; Clark et al., 2020), suggest that Tcu is likely Early Miocene to Late Eocene (Anderson and McKean, 2018); estimated thickness in the quadrangle 500 to 1600 feet (150–500 m); to the east in the Fort Douglas quadrangle, exposed thickness is at least 4200 feet (1400 m) and based on Van Horn and Crittenden's (1987) cross section, the thickness of the unit is about 8500 feet (2600 m).

Unconformity

Tv **Volcaniclastic conglomerate** (Late to Middle Eocene) – Poorly to moderately cemented volcaniclastic conglomerate, with angular to subrounded clasts; dark-gray to grayish-red-purple volcanic rock with light-gray matrix of low-density ash and medium- to coarse-grained volcanic sand; intermediate geochemical composition of five clasts include latite, trachydacite, and dacite (Figure 3; samples SLCN2014-279 [2 clast], SLCN2014-283[2 clast], and SLCN2014-284; McKean, 2017); volcanic clasts have variety of phenocrysts assemblages (including biotite, plagioclase, hornblende, and/or sanidine); clasts are pebble to boulder in size, largest clast 5 feet (1.5 m), one rounded 6-inch (15 cm) quartzite clast that was observed within the unit (see also Van Horn, 1981); typically forms dark, cobble-strewn slopes; mapped in City Creek Canyon and on the northwestern slope of the Salt Lake salient near the Springhill landslide; the volcanic clasts were most likely deposited in mud and debris flows along the flanks of a volcanic center; the lower contact is marked by the appearance of volcanic clasts in float; outcrop pattern is lenticular and discontinuous between the tuffaceous strata (Tt) and the upper conglomerate (Tcu); Van Horn (1981) reported a zircon fission track age of 35.3 ± 1.6 Ma, and biotite K-Ar ages of 37.7 ± 1.1 and 38.8 ± 1.2 Ma, all from volcanic clasts; Mann (1974) reported biotite K-Ar ages of 50.9 ± 2.0 Ma and an amphibole K-Ar age of 55.7 ± 2.6 Ma from exposures in City Creek Canyon; the volcaniclastic conglomerate overlies the Middle to Early Eocene tuffaceous strata (Tt), confirming the 50 to 55 Ma ages are too old; $^{40}Ar/^{39}Ar$ analysis of biotite from a dacite clast (sample SLCN2014-283-1) yielded a 39.52 ± 0.19 (1σ) Ma isochron age (McKean and NIGL, 2016); based on stratigraphic position and the Late to Middle Eocene age, the volcaniclastic conglomerate may be time-correlative with the Keetley Volcanics near Park City (Van Horn and Crittenden, 1987; Biek, 2022; Biek et al., 2022) or the Eocene volcanic rocks in the southeast Oquirrh and Traverse Mountains (Clark et al., 2020, 2023); thickness is highly variable, estimated 0 to 500 feet (0–150 m).

Minor Unconformity

Tt **Tuffaceous strata** (Middle to Early Eocene) – Tuffaceous, light-gray to light-red siltstone, mudstone, sandy limestone, limestone, sandstone, and interbedded conglomerate; also contains interbedded ash beds; commonly contains biotite; lithologies interfinger and change rapidly, both horizontally and vertically, but these relationships are rarely exposed due to the slope forming nature of the unit; upper part is generally dominated by tuffaceous white to light-gray siltstone, mudstone, limestone, and sandy limestone, locally contains conglomerate beds with Paleozoic to Mesozoic clasts with occasional Tertiary volcanic clasts; the lower part generally contains light-gray to light-red sandstone and interbedded pebble-conglomerate that fines up section; locally, the sandstone has an ashy component that also contains grains of biotite, amphibole, and lithics; gray and red-colored conglomerate beds are composed of clasts of Paleozoic limestone, tan sandstone, light-red sandstone, and quartzite with a sandy matrix; other conglomerate beds are composed of Paleozoic and Mesozoic limestone and sandstone, volcanic, and quartzite clasts with a white ashy matrix and are found near the mouth of City Creek Canyon (SW¼, section 30, T. 1 N., R. 1 E.) and in the Fort Douglas quadrangle (Anderson et al., 2024); upper part is commonly altered to clay and susceptible to landsliding; numerous historical landslides failed in this unit including the Springhill and Parkway Drive landslides, and landslides in City Creek Canyon; the lower contact is unconformable or gradational; gradational contacts commonly mapped where sandstone facies dominate over conglomerate and sandstone beds have a tuffaceous component (e.g., presence of biotite and euhedral feldspars); Van Horn (1981) reported an unpublished K-Ar biotite ages from a water-laid tuff of 45.0 ± 1.4 Ma and a zircon fission track age of 37.4 ± 1.6 Ma; a U-Pb detrital zircon sample from a tuffaceous siltstone yielded a maximum depositional age of 44.75 ± 0.29 Ma (2σ) (sample SLCN2014-285, McKean et al., 2016); based on stratigraphic position and age, the unit may correlate with the Fowkes Formation exposed to the northeast near Evanston, Wyoming (Coogan and King, 2016), and Cache Valley, Utah (Oaks et al., 1999); thickness highly variable, estimated 30 to 1200 feet (10–360 m).

Unconformity

Tcl **Lower conglomerate** (Eocene to Paleocene?) – Mostly light-gray to gray, well-cemented conglomerate, composed of sand, pebbles, cobbles and boulders; contains thin discontinuous lenses of fine- to coarse-grained quartz and lithic sandstone; mostly clast-supported with minor amount of sandy matrix; clasts are rounded to subangular and are composed of Paleozoic limestone, sandstone, quartzite, and chert; forms cliffs and steep slopes; exposed on the western-most part of the Salt Lake salient and near Twin Peaks in the neighboring Fort Douglas quadrangle; lower contact is unconformable, shows evidence of considerable paleotopography developed on underlying Paleozoic rocks and is commonly marked by a deeply weathered, red-colored zone that may represent paleosols and regolith development prior to deposition (see Van Horn, 1981); McKean et al. (2016) report a U-Pb detrital zircon maximum depositional age of 48.47 ± 0.76 Ma from a sandstone bed near the top of the unit (sample SLCN2014-286); while occupying a similar tectono-stratigraphic position to the Wasatch Formation (Tw) in the neighboring Bountiful Peak quadrangle (Anderson, 2023) and yielding a maximum depositional age reasonable of the Wasatch Formation, the clast composition differs markedly from nearby Tw exposures (this unit is less heterolithic than Tw), therefore we interpret this as not equivalent to Tw; may correlate with Bryant's (1990) Oligocene-Eocene(?) Conglomerate (map unit Toc) exposed to the east in the Wasatch Range (see also map unit Toc unit of Biek, 2022; Biek et al., 2022), which overlies Tw and in its upper part interfingers with volcaniclastic units similar in age to those of this map's Tt and Tv; estimated unit thickness 600 to 1150 feet (180–350 m).

Major unconformity

A red weathered zone or paleosol developed on Paleozoic bedrock before deposition of the lower conglomerate (Tcl). Van Horn (1981) described the zone as a reddish-brown weathering silt and clay that contains jumbled blocks of Paleozoic limestone and conglomerate boulders, up to 10 feet (3 m) thick. This red soil may represent a terra rossa soil developed on the folded Paleozoic limestones and dolomites following Sevier deformation. Numerous vugs and small caves are found in the underlying Paleozoic units. Perhaps these cavities and red soil are evidence for paleo karst processes or hydrothermal alteration along the Warm Springs fault. Whether sourced from the terra rossa or hydrothermal alteration or both, the red staining is exposed in the aggregate mining pit walls on the west side of the Salt Lake salient and where leached out of the rock, it is deposited down the pit walls as a coating.

PALEOZOIC

MISSISSIPPIAN

Mdo, Mdo?

Doughnut Formation (Late Mississippian) – Only mapped as stacked units, but well-exposed in quarries on the west side of the Salt Lake salient where surficial cover has been removed by mining; light to dark blue-gray fossiliferous limestone, shaley limestone, and cherty limestone; includes crinoids, bivalves, rugose corals, brachiopods, bryozoans, and fossil hash; thin to medium-bedded with laminar, wavy, and cross-bedded bed sets; locally, beds are highly silicified and very dense; nodular to dark gray to black chert; forms slopes and ledges; located at the mouth of Hell Canyon in the Staker Parsons Falcon Ridge Pit and other small isolated outcrops; the lower contact is a detachment fault mapped above the highest sandstone of the Humbug Formation; to the east, in the Fort Douglas quadrangle, the basal ~150 feet (50 m) is composed of shale and shaley limestone that forms a swale between the Humbug Formation below and the main limestone body of the Doughnut Formation above (unit Mdos of Van Horn and Crittenden, 1987); basal shale is not identified in this quadrangle but may be cut out by a regional detachment fault as shown on cross section B-B'; Late Mississippian age from Baker and Crittenden (1961); in the Morgan quadrangle to the northeast, Coogan et al. (2015) reported a Morrowan (Early Pennsylvanian) palynomorph age on the upper Doughnut, but strata like their clastic-poor upper Doughnut have not been identified during this mapping; queried where unit designation uncertain, may include some undifferentiated Pennsylvanian Round Valley Limestone; exposed thickness at least 800 feet (240+ m); in the Fort Douglas quadrangle, Van Horn and Crittenden (1987) reported a thickness of 1000 feet (330 m), upper part covered by lacustrine gravel and lower conglomerate (Tcl); Bryant (1990) reported a thickness of 425 feet (130 m) in the Wasatch Range.

Mh **Humbug Formation** (Late Mississippian) – Only mapped as stacked units, but well-exposed in quarries on the west side of the Salt Lake salient where surficial cover has been removed by mining; interbedded medium to dark blue-gray limestone and light-brown calcareous quartz sandstone and orthoquartzite; medium-bedded; limestone is fine to medium grained, with crinoids, rugose corals, and shell hash; locally dolomitic; sandstone is fine to medium grained with well-sorted and rounded grains, low-angle cross-stratification, and lenticular beds; forms ledges and slopes; lower contact with the Deseret Limestone is gradational and is placed at the base of the first sandstone bed; regional age from Morris and Lovering (1961); estimated thickness between 1000 and 1400 feet (300–425 m); in the Fort Douglas quadrangle, Van Horn and Crittenden (1987) reported a unit thickness of 1050 feet (320 m); in the Salt Lake City 30′ x 60′ quadrangle Bryant (1990) reported a thickness of 400 to 920 feet (120–280 m).

Md **Deseret Limestone** (Late to Early Mississippian) – Only mapped as stacked units, but well-exposed in quarries on the west side of the Salt Lake salient where surficial cover has been removed by mining; medium- to dark-gray shaley limestone, cherty limestone, and fossiliferous limestone that is medium to very thick bedded; upper part is very thick bedded limestone containing dark gray, black, and brown nodular to bedded chert and beds of coquina (shell hash); shell hash is composed of fragments of fossilized broken shells, crinoid columnals, and corals oriented into laminae and cross-beds; the chert is mostly nodular with some bedded chert, most of the chert is dark gray to black and brown in color; intact fossils include rugose corals, crinoids, bryozoans; lower part (Delle Phosphatic Member, mapped separately in the neighboring Fort Douglas quadrangle [Anderson et al., 2024]) is a black carbonaceous shale/shaley limestone that is rarely exposed and may be absent in this quadrangle due to structural thinning; forms slopes and ledges; lower contact is placed at the change from bedded cherty limestone of the Gardison Limestone to shaley and cherty limestone of the Deseret Limestone (Md); regional age from Sandberg and Gutschick (1979); estimated thickness between 500 and 800 feet (150–250 m); in the Fort Douglas quadrangle, Van Horn and Crittenden (1987) reported a unit thickness of 460 feet (140 m); in the Salt Lake City 30′ x 60′ quadrangle Bryant (1990) report a thickness of 460 to 970 feet (140–295 m).

Mg **Gardison Limestone** (Early Mississippian) – Only mapped as a stacked unit, but well-exposed in quarries on the west side of the Salt Lake salient where surficial cover has been removed by mining; medium-gray to dark-blue-gray limestone, cherty limestone, and fossiliferous limestone that is medium- to very thick bedded; chert is present as black, irregularly shaped nodules and thin, discontinuous beds; Van Horn and Crittenden (1987) reported brachiopods, corals, and bryozoans; the lower contact is disconformable and is marked by the presence of more resistant limestone with abundant Mississippian fossil assemblage compared to the underlying limestone and the shaley limestone of the Pinyon Peak Limestone (Dpp); late Kinderhookian to early-middle Osagean from conodonts in the Lakeside Mountains (Silberling and Nichols, 1992), regional age from Morris and Lovering (1961); estimated thickness 850 to 950 feet (260–290 m); in the Fort Douglas quadrangle, Van Horn and Crittenden (1987) reported a thickness of 660 feet (200 m); in the Salt Lake City 30′ x 60′ quadrangle Bryant (1990) reported a thickness of 660 feet (200 m) for the unit in the Wasatch Range.

Unconformity

DEVONIAN

Dpp **Pinyon Peak Limestone** (Late Devonian) – Only mapped as a stacked unit, but well-exposed in the quarries on the west side of the Salt Lake salient where surficial cover has been removed by mining; medium to light blue-gray, commonly with a faint pink hue, limestone and argillaceous limestone, thin to medium bedded, and fossiliferous; forms slopes; the lower contact is likely conformable and placed at the appearance of the first argillaceous limestone beds of the Pinyon Peak Limestone above uppermost quartzite or sandy dolomites of the Stansbury Formation (Dst); Gosney (1982) described conodonts from this location from the Pinyon Peak Limestone and Fitchville Formation, we did not observe Fitchville Formation at this location, but some could be mapped as Pinyon Peak Limestone or Gardison Limestone; late Famennian age from conodonts in the Lakeside Mountains (Silberling and Nichols, 1992), regional age from Morris and Lovering (1961); estimated thickness 130 and 200 feet (40–60 m); in the Fort Douglas quadrangle estimated thickness of 160 to 200 feet (50–60 m) (Anderson et al., 2024); in the Salt Lake City 30′ x 60′ quadrangle Bryant (1990) reported a thickness of 160 to 200 feet (50–60 m) for the unit north and east of Salt Lake City.

Dst **Stansbury Formation** (Late Devonian) – Only mapped as a stacked unit, but well-exposed on the west side of the Salt Lake salient where surficial cover has been removed by mining; pale gray to white to yellowish-gray sandstone, silty limestone, and shaley sandstone composed of fine- to coarse-grained quartz (Van Horn and Crittenden, 1987; Bryant, 1990); forms slopes and ledges; the lower contact with the Cambrian limestone and shale (Ꞓu) is unconformable and represents uplift and erosion across the Tooele arch (Rigby, 1959; Trexler, 1992); various fossil data indicate the formation ranges from early Kinderhookian to late Famennian in age (Sandberg and Gutschick, 1979; Mamet, in Trexler, 1992; Stamm, in Silberling and Nichols, 1992); estimated thickness is 270 to 300 feet (80–90 m); estimated thickness from the Fort Douglas quadrangle is 460 feet (140 m) (Anderson et al., 2024); in the Salt Lake City 30′ x 60′ quadrangle Bryant (1990) reported a thickness of 500 feet (150 m) for the unit north and east of Salt Lake City.

Major Unconformity (Stansbury uplift and Tooele arch; see Hintze, 1959; Rigby, 1959; Morris and Lovering, 1961, and references therein; Rigby and Clark, 1962; Tooker, 1999; Ethington et al., 2016)

CAMBRIAN

Ꞓu **Cambrian strata, undivided** (Late to Middle Cambrian) – Only mapped as stacked units, but exposed on the west side of the Salt Lake salient where surficial cover has been removed by mining; light to dark blue-gray dolomite, limestone, and sandy limestone, mottled with grayish-yellow shale; thin to medium bedded; brecciated and altered along fault zones; forms ledges and cliffs; unit likely includes Late Cambrian St. Charles Formation and Nounan Formation, and Middle Cambrian Bloomington Formation and Maxfield Limestone; undivided here due to the highly fractured, faulted, and concealed nature of outcrops; a detachment in the Cambrian section present in the Fort Douglas quadrangle was not observed here due to the brecciated and altered nature of the bedrock but may be present; Late to Middle Cambrian age based on various trilobite and conodonts fossils (Rigo, 1968; Taylor, et al., 1981; Oviatt,1986); exposed thickness at least 1200 feet (360+ m); in the adjacent Fort Douglas and Bountiful Peak quadrangles, the St. Charles Formation is 440 to 520 feet (130–160 m) thick, the Nounan Formation is 550 to 590 feet (160–180 m) thick, the Bloomington Formation is 200 feet (60 m) but may be structurally thickened to as much as 350 feet (110 m) thick, and the Maxfield Limestone is a between 610 and 830 feet (185–250 m) thick (Anderson, 2023; Anderson et al., 2024).

Ꞓo **Ophir Formation** (Middle Cambrian) – Not exposed in the quadrangle, shown on cross section only. In the adjacent Fort Douglas quadrangle, Van Horn and Crittenden (1987) reported a thickness of 250 to 400 feet (75–125 m) and in Bountiful Peak quadrangle Anderson (2023) reported a thickness of 300 to 380 feet (90–115 m).

Ꞓt **Tintic Quartzite** (Middle to Early Cambrian?) – Not exposed in the quadrangle, shown on cross section only. In the adjacent Fort Douglas quadrangle, Van Horn and Crittenden (1987) reported a thickness of 1970 feet (600 m), and in Bountiful Peak quadrangle Anderson (2023) reported a thickness of 1500 to 1970 feet (450–600 m).

SUBSURFACE UNITS

Quaternary deposits – Shown on cross section only. Likely consists of principally undivided alluvial and lacustrine sediments. Thickness of unconsolidated deposits estimated from geophysical and deep and shallow borehole data (Arnow and Mattick, 1968; Arnow et al., 1970; Van Horn, 1981; Radkins et al., 1989; and Hill et al., 1990). Berry and Crawford (1932, reported in Arnow and Mattick, 1968) reported Pleistocene molluscs at 884 feet in their Western Petroleum Drilling Co. #1 well. To the west in the Baileys Lake quadrangle, the top of Quaternary-Tertiary contact in the Saltair #1 well is at a depth of 1288 feet (393 m) and in the Saltair #2 well, the contact is at a depth of 1086 feet (331 m) (McKean and Hylland, 2019a; Willis and Jensen, 2000). Radkins et al. (1989) R-1 seismic reflector, combined with available exploration well log data, were used to interpret the depth of the Quaternary-Neogene and Paleogene contact on cross section A-A'.

Neogene-Paleogene strata – Shown on cross section only. Descriptions in Cook and Berg (1961), derived from Hansen and Scoville (1955) and Eardley and Hass (1936), of Western Petroleum Drilling Co. #1 well (Table 2) indicate that the well penetrated Tertiary marl, volcanic ash and tuff, including a 2.5-foot (<1 m) bed of tuff, at a depth of 1308 feet (400 m). The electronic logs for the Gillmor Fee 1 well (Table 2) indicate high gamma ray readings from about 3600 to 4500 feet (1100–1370 m), which we interpret to represent Neogene-Paleogene volcanic rocks. Based on the well interpretation, the Neogene-Paleogene to Mesozoic and Paleozoic contact on cross section A-A' is drawn slightly deeper than Radkins et al.'s (1989) R-2 seismic reflector that depicts the same contact. The R-11 seismic line of Radkins et al. (1989) shows an angular unconformity between the Neogene-Paleogene strata and Mesozoic and Paleozoic strata.

Unconformity

Mesozoic and Paleozoic strata? – Shown on cross section only. Mesozoic and Paleozoic strata are likely present in the subsurface of the Salt Lake Valley based on structural relationships along the Wasatch fault zone. These rocks have been depicted on previously published cross sections of the valley (Van Horn and Crittenden, 1987; Doelling et al., 1990; Solomon et al., 2007; McKean and Hylland, 2019a; Clark et al., 2020). Electronic logs for the Gillmor Fee 1 well (Table 2) indicate a possible depth for Mesozoic and Paleozoic strata from 4500 feet (1372 m) to the total depth of 6120 feet (1865 m). Radkins et al.'s (1989) R-3 seismic reflector was also used to interpret the depth of the Mesozoic and Paleozoic to Precambrian? contact on cross section A-A'.

Unconformity

Precambrian metamorphic bedrock and Farmington Canyon Complex (Precambrian) – Shown on cross section only. To the west in the Baileys Lake quadrangle, the Neogene-Paleogene to Precambrian contact in the Saltair #1 well is at a depth of 3070 feet (936 m) and in the Saltair #2 well, the contact is interpreted to be below the 3000-foot (914 m) interval (McKean and Hylland, 2019a; Willis and Jensen, 2000). To the west, the Whitlock-Morton Salt Co. #1 well is in the easternmost part of the Antelope Island South quadrangle; the lithologic notes of the well indicate that the depth to Precambrian metamorphic bedrock is at 3654 feet (1113 m) (Arnow and Mattick, 1968; Ritzma, unpublished data UGS files, 1975; Willis and Jensen, 2000), the rock encountered is likely Farmington Canyon Complex, but may include some Neoproterozoic bedrock as well, like what is on Antelope Island (Doelling et al., 1990). In the western part of the Baileys Lake quadrangle, the Neogene-Paleogene strata appear to be in direct contact with Precambrian bedrock as shown on cross section B-B' of McKean and Hylland (2019a). In the eastern part of the Baileys Lake quadrangle and the western Salt Lake City North quadrangle, Radkins et al.'s (1989) R-3 seismic reflector shows an eastward thickening of strata (potentially Mesozoic to Paleozoic strata) overlying the Precambrian bedrock. Geology of the Wasatch Range, Oquirrh Mountains, and Antelope Island, imply that major thrust faults of the Sevier orogeny are also present in the Precambrian to Mesozoic strata in the subsurface, but their location and exact nature are uncertain and are not represented on cross section A-A'. The Precambrian bedrock under the Salt Lake salient is likely Farmington Canyon Complex with no Neoproterozoic bedrock as seen to the immediate east (Anderson, 2023; and Anderson et al., 2024). See cross sections and discussions of Van Horn and Crittenden (1987), Bryant (1988, 1990), Willis et al. (2010), Yonkee and Weil (2011), McKean and Hylland (2019a), Clark et al. (2020), and Kleber et al. (2021) for more details regarding regional thrust faults that may be present in the subsurface.

ACKNOWLEDGMENTS

This geologic map was funded by the Utah Geological Survey and the U.S. Geological Survey, National Cooperative Geologic Mapping Program, through USGS STATEMAP award number G13AC00169 (2013–2014). Discussions with many individuals helped in the development of this map and report, including local consultants David Simon, Greg Schlenker, Doug Hawkes, and Peter Doumit; Chris DuRoss (USGS): Steve Bartlett (University of Utah); Lee Liberty (Boise State University); and UGS staff Jon King (retired), Mike Hylland (retired), Emily Kleber, Adam Hiscock, Greg McDonald, Doug Sprinkel (retired), and Grant Willis (retired). UGS staff members Donald Clark, Stefan Kirby, Steve Bowman, Stephanie Carney, Darlene Batatian, and Bill Keach improved this map and report through their reviews. UGS interns Kirk Schleiffarth and Sofia Agopian assisted with fieldwork and sampling. Kent Brown (retired UGS) assisted with digital photogrammetry for stereo photo mapping. Corey Unger (formerly UGS), Kent Brown (retired UGS), and Jay Hill (UGS) provided technical advice and assistance with map and figures. We are grateful to all the property owners who allowed us access to their property for field mapping purposes.

REFERENCES

AGEC, Applied Geotechnical Engineering Consultants, Inc., 1999, Surface fault rupture hazard investigation and site specific liquefaction evaluation, Rose Wagner Phase II Dance Theatre, 150 West Broadway, Salt Lake City, Utah: unpublished consultant report prepared for Salt lake County c/o Beneco Enterprises, Inc., variously paginated.

AGRA Earth & Environmental, Inc., 1997, Report, fault rupture hazard study, proposed 80-acre office park, between 2200 West and West Interstate I-215 and between 800 and 1200 North, Salt Lake City, Utah: unpublished consultant report prepared for The Boyer Company, 18 p.

Anderson, L.R., Keaton, J.R., Aubrey, K., and Ellis, S., 1994, Liquefaction potential map for Davis County, Utah, complete technical report: Utah Geological Survey Contact Report 94-7, 50 p., 8 plates, https://doi.org/10.34191/CR-94-7.

Anderson, Z.W., 2023, Geologic map of the Bountiful Peak quadrangle, Davis and Morgan Counties, Utah: Utah Geological Survey Map 289DM, 17 p., 1 plate, https://doi.org/10.34191/M-298DM.

Anderson, Z.W., and McKean, A.P., 2018, New insights on the structural and basin evolution of the Salt Lake salient and Wasatch fault zone near Salt Lake City, Utah [abs.]: Geological Society of America Abstracts with Programs, v. 50, no. 5, https://doi.org/10.1130/abs/2018RM-313664.

Anderson, Z.W., McKean, A.P., and Yonkee, A.W., 2024, Interim geologic map of the Fort Douglas quadrangle, Salt Lake, Davis, and Morgan Counties, Utah: Utah Geological Survey Open-File Report 767, 32 p., 2 plates, scale 1:24,000, https://doi.org/10.34191/OFR-767.

Applied Geotechnical Engineering Consultants, Inc., 1994, Environmental impact report, Scenic Hills, No. 3 PUD, North Salt Lake City, Utah: unpublished consultant report prepared for Hill, Jamison and Associates, Inc., 57 p.

Armstrong, P.A., Taylor, A.R., and Ehlers, T.A., 2004, Is the Wasatch fault footwall (Utah, United States) segmented over million-year time scales?: Geology, v. 32, no. 5, p. 385–388.

Arnow, T., and Mattick, R.E., 1968, Thickness of valley fill in the Jordan Valley east of the Great Salt Lake, Utah, *in* Geological Survey Research, 1968: U.S. Geological Survey Professional Paper 600-B, p. B79–82.

Arnow, T., and Stephens, D., 1990, Hydrologic characteristics of the Great Salt Lake, Utah—1847–1986: U.S. Geological Survey Water-Supply Paper 2332, 32 p., scale 1:125,000.

Arnow, T., Van Horn, R., and LaPray, R., 1970, The pre-Quaternary surface in the Jordan Valley, Utah, *in* Geological Survey Research, 1970: U.S. Geological Survey Professional Paper 700-D, p. D257–261.

Ashland, F.X., 2003, Characteristics, causes, and implications of the 1998 Wasatch Front landslides, Utah; Utah Geological Survey Special Study 105, 49 p., https://doi.org/10.34191/SS-105.

Atwood, G., 2006, Shoreline superelevation— evidence of coastal processes of Great Salt Lake, Utah: Utah Geological Survey Miscellaneous Publication 06-9, 231 p., https://doi.org/10.34191/MP-06-9.

Atwood, G., and Mabey, D.R., 1995, Flooding hazards associated with Great Salt Lake, *in* Lund, W.R., editor, Environmental and engineering geology of the Wasatch Front region: Utah Geological Association Publication 24, p. 483–494.

Baker, A.A., and Crittenden, M.D., Jr., 1961, Geology of the Timpanogos Cave quadrangle, Utah: U.S. Geological Survey Geologic Quadrangle Map GQ-132, 1 plate, scale 1:24,000.

Best, M.G., and Christiansen, E.H., 1991, Limited extension during peak Tertiary volcanism, Great Basin of Nevada and Utah: Journal of Geophysical Research, v. 96, p. 13,509–13,528.

Biek, R.F., 2022, Geologic map of the Park City East quadrangle, Summit and Wasatch Counties, Utah: Utah Geological Survey Map 296DM, 23 p., 2 plates, scale 1:24,000, https://doi.org/10.34191/M-296DM.

Biek, R.F., Yonkee, W.A., and Loughlin, W.D., 2022, Geologic map of the Park City West quadrangle, Summit and Salt Lake Counties, Utah: Utah Geological Survey Map 297DM, 21 p., 2 plates, scale 1:24,000, https://doi.org/10.34191/M-297DM.

Berry, E.G., and Crawford, A.L., 1932, Preliminary notes on the Mollusca of Lake Bonneville: Utah Academy of Sciences, Proceedings, v. 9, p. 53–54.

Bowman, S.D., Castleton, J.J., and Elliott, A.H., 2009, New geologic hazards mapping in Utah: Utah Geological Survey, Survey Notes, v. 41, no. 3, p. 1–3, https://doi.org/10.34191/SNT-41-3.

Bowman, S.D., Hiscock, A.I., and Unger, C.D., 2015, Paleoseismology of Utah, Volume 26—Compilation of 1970s Woodward-Lundgren & Associates Wasatch fault investigation reports and low-sun-angle aerial photography, Wasatch Front and Cache Valley, Utah and Idaho: Utah Geological Survey Open-File Report 632, 8 p., 6 plates, https://doi.org/10.34191/OFR-632.

Bowman, S.D., and Lund, W.R., editors, 2020, Guidelines for investigating geologic hazards and preparing engineering-geology reports, with a suggested approach to geologic-hazard ordinances in Utah, second edition: Utah Geological Survey Circular 128, 170 p., 5 appendices, https://doi.org/10.34191/C-128.

Bronk Ramsey, C., 2009, Bayesian analysis of radiocarbon dates: *Radiocarbon, v. 51,* no. 1, p. 337–360.

Bryant, B., 1988, Geology of the Farmington Canyon Complex, Wasatch Mountains, Utah: U.S. Geological Survey Professional Paper 1476, 54 p., 1 plate, scale 1:50,000.

Bryant, B., 1990, Geologic map of the Salt Lake City 30′ x 60′ quadrangle, north-central Utah, and Uinta County, Wyoming: U.S. Geological Survey Miscellaneous Investigations Series Map I-1944, 2 plates, scale 1:100,000.

Castleton, J.J., and McKean, A.P., 2012, The Utah Geological Survey geologic hazards mapping initiative, *in* Hylland, M.D., and Harty, K.M., editors, Selected topics in engineering and environmental geology in Utah: Utah Geological Association Publication 41, p. 51–67.

Christenson, G.E., and Ashland, F.X., 2007, A plan to reduce losses from geologic hazards in Utah—recommendations of the Governor's Geologic Hazards Working Group 2006–2007: Utah Geological Survey Circular 104, 30 p., https://doi.org/10.34191/C-104.

Clark, D.L., Kirby, S.M., and Oviatt, C.G., 2023, Geologic map of the Rush Valley 30' X 60' quadrangle, Tooele, Utah, and Salt Lake Counties, Utah: Utah Geological Survey Map 294DM, 46 p., 2 appendices, 3 plates, scale 1:62,500, https://doi.org/10.34191/M-294DM.

Clark, D.L., Oviatt, C.G., and Dinter, D.A., 2020, Geologic map of the Tooele 30' X 60' quadrangle, Tooele, Salt Lake, and Davis Counties, Utah: Utah Geological Survey Map 284DM, 48 p., 2 appendices, 4 plates, scale 1:62,500, https://doi.org/10.34191/M-284DM.

Cluff, L., Brogran, G., and Glass, C., 1970, Wasatch fault, northern portion, earthquake fault investigation and evaluation, a guide to land use planning: Oakland, California, Woodward-Clyde and Associates, unpublished consultant's report for the Utah Geological and Mineralogical Survey, variously paginated.

Constenius, K.N., 1996, Late Paleogene extensional collapse of the Cordilleran foreland fold and thrust belt: Geological Society of America Bulletin, v. 108, p. 20–39.

Coogan, J.C., King, J.K., and McDonald, G.N., 2015, Interim geologic map of the Morgan quadrangle, Morgan County, Utah: Utah Geological Survey Open-File Report 643, 30 p., 2 plates, scale 1:24,000, https://doi.org/10.34191/OFR-643.

Coogan, J.C., and King, J.K., 2016, Interim geologic map of the Ogden 30' x 60' quadrangle, Box Elder, Cache, Davis, Morgan, Rich, and Summit Counties, Utah, and Uinta County, Wyoming: Utah Geological Survey Open-File Report 653DM, 1:62,500 scale, 3 plates, 147 p., https://doi.org/10.34191/OFR-653DM.

Cook, K.L., and Berg, J.W., 1961, Regional gravity survey along the central and southern Wasatch Front, Utah: U.S. Geological Survey Professional Paper 316-E, plate 13, p. 75–89.

Currey, D.R., and James, S.R., 1982, Paleoenvironments of the northeastern Great Basin and northeastern Basin Rim region—a review of geological and biological evidence, *in* Madsen, D.B., and O'Connell, J.F., editors, Man and environment in the Great Basin: Society for American Archeology Papers, no. 2, p. 27–52.

DeCelles, P.G., 2004, Late Jurassic to Eocene evolution of the Cordilleran thrust belt and foreland basin system, western U.S.A.: American Journal of Science, v. 304, p. 105–168.

Dickinson, W.R., 2006, Geotectonic evolution of the Great Basin: Geosphere, v. 2, no. 7, p. 353–368.

Doelling, H.H., and Willis, G.C., 1995, Guide to authors of geologic maps and text booklets of the Utah Geological Survey: Utah Geological Survey Circular 89, 98 p., https://doi.org/10.34191/C-89.

Doelling, H.H., Willis, G.C., Jensen, M.E., Hecker, S., Case, W.F., and Hand, J.S. (with contributions by Davis, F.D., Klauk, R.H., Gwynn, J.W., Bishop, C.E., and Atwood, G.), 1990, Geologic map of Antelope Island, Davis County, Utah: Utah Geological Survey Map 127, 27 p., 2 plates, scale 1:24,000, https://doi.org/10.34191/M-127. (Subsequently published in 2018 as Utah Geological Survey Digital Reproduction M-127DR, https://doi.org/10.34191/M-127DR.)

DuRoss, C. B., and Hylland, M. D., 2014, Evaluating surface faulting chronologies of graben-bounding faults in Salt Lake Valley, Utah–new paleoseismic data from the Salt Lake City segment of the Wasatch fault zone and the West Valley fault zone, *in* Paleoseismology of Utah, DuRoss, C.B., and Hylland, M.D., editors; Utah Geological Survey Special Study 149, v. 24, 71 p., https://doi.org/10.34191/SS-149.

DuRoss, C.B., and Hylland, M.D., 2015, Synchronous ruptures along a major graben-forming fault system—Wasatch and West Valley fault zones, Utah: Bulletin of the Seismological Society of America, v. 105, no. 1, p. 14–37.

DuRoss, C.B., Personius, S.F., Crone, A.J., Olig, S.S., Hylland, M.D., Lund, W.R., and Schwartz, D.P., 2016, Fault segmentation—new concepts from the Wasatch fault zone, Utah, USA: Journal of Geophysical Research Solid Earth, v. 121, p. 1–27.

Eardley, A.J., and Hass, M., 1936, Oil and gas possibilities in the Great Salt Lake basin: Utah Academy of Sciences, Arts, and Letters, Proceedings, v. 13, p. 61–80.

Earthquake Engineering Research Institute, Utah Chapter, 2015, Scenario for a magnitude 7.0 earthquake on the Wasatch fault–Salt Lake City segment—hazards and loss estimates: Earthquake Engineering Research Institute, Utah Chapter, 53 p., Online, https://dem.utah.gov/wp-content/uploads/sites/18/2015/03/RS1058_EERI_SLC_EQ_Scenario.pdf, accessed, February 11, 2022.

Ethington, R.L., Ritter, S.M., Clark, D.L., and Kowallis, B.J., 2016, Conodont biostratigraphy of the Ordovician Opohonga Limestone in west-central Utah: Palaios, v. 31, p. 221–230.

Francis, M., Yeh, H., Dinter, D., Hong Kie Thio, and Olig, S., 2011, Tsunami and seiche risk framework for the Great Salt Lake, *in* Wallendorf, L.A., Jones, C., Ewing, L., and Battalio, B., Solutions to Coastal Disasters Conference 2011, proceedings of the 2011 solutions to coastal disasters conference Jun 26, 2011, Anchorage, Alaska, p. 376–395.

Fred C. Hart Associates, Inc., 1980, Assessment of a hazardous waste disposal site at Rose Park, Salt Lake City, Utah: Report prepared for U.S. Environmental Protection Agency Technical Assistance Panels Program, dated May, 1980, variously paginated, Online https://www.epa.gov/nscep, accessed August 7, 2019.

Gilbert, G.K., 1890, Lake Bonneville: U.S. Geological Survey Monograph 1, 438 p.

Gilbert, G.K., 1928, Studies of Basin Range Structure: U.S. Geological Survey Professional Paper 153, 92 p., https://doi.org/10.3133/pp153.

Giraud, R.E., 1999, Reconnaissance of building distress and ground movement in the Springhill Circle area, North Salt Lake, Davis County, Utah, *in* McDonald, G.N., compiler, Technical reports for 1998, Applied Geology Program: Utah Geological Survey Report of Investigation 242, p. 60–75, https://doi.org/10.34191/RI-242.

Godsey, H.S., Currey, D.R., and Chan, M.A., 2005, New evidence for an extended occupation of the Provo shoreline and implications for regional climate change, Pleistocene Lake Bonneville, Utah, USA: Quaternary Research, v. 63, p. 212–223.

Godsey, H.S., Oviatt, C.G., Miller, D.M., and Chan, M.A., 2011, Stratigraphy and chronology of offshore to nearshore deposits associated with the Provo shoreline, Pleistocene Lake Bonneville, Utah: Palaeogeography, Palaeoclimatology, Palaeoecology, v. 310, nos. 3–4, p. 442–450.

Gori, P.L., and Hays, W.W., editors, 1992, Assessment of regional earthquake hazards and risk along the Wasatch Front, Utah: U.S. Geological Survey Professional Paper, variously paginated.

Gosney, T.C., 1982, Conodont biostratigraphy of the Pinyon Peak Limestone and the Fitchville Formation, Late Devonian-Early Mississippian, North Salt Lake City, Utah: Brigham Yong University Geology Studies, v. 29, part 2, p. 27–39.

Hansen, G.H., and Scoville, H.C., 1955, Drilling records for oil and gas in Utah: Utah Geological and Mineral Survey Bulletin 50, 110 p., https://doi.org/10.34191/B-50.

Harty, K.M., and Christenson, G.E., 1988, Flood hazard from lakes and failure of dams in Utah: Utah Geological and Mineral Survey Map 111, 8 p., 1 plate, scale 1:750,000, https://doi.org/10.34191/M-111.

Harty, K.M., and Lowe, M., 2003, Geologic evaluation and hazard potential of liquefaction-induced landslides along the Wasatch Front, Utah: Utah Geological Survey Special Study 104, 40 p., 16 plates, https://doi.org/10.34191/SS-104.

Hecker, S., Harty, K.M., and Christenson, G.E., 1988, Shallow ground water and related hazards in Utah: Utah Geological and Mineral Survey Map 110, 17 p., 2 plates, scale 1:750,000, https://doi.org/10.34191/M-110.

Hedge, C.E., Stacey, J.S., and Bryant, B., 1983, Geochronology of the Farmington Canyon Complex, Wasatch Mountains, Utah, *in* Miller, D.M., Todd, V.R., and Howard, K.A., editors, Tectonics and stratigraphic studies of the eastern Great Basin: Geological Society of America Memoir 157, p. 37–44.

Hill, B.V., 2018, Analysis of the Parkway Drive landslide, North Salt Lake, UT: Logan, Utah State University, M.S. thesis, 63 p.

Hill, J., Benz, H., Murphy, M., and Schuster, G., 1990, Propagation and resonance of SH waves in the Salt Lake Valley, Utah: Bulletin of the Seismological Society of America, v. 80, no. 1, p. 23–42.

Hintze, L.F., 1959, Ordovician regional relationships in north-central Utah and adjacent areas, *in* Williams, N.C., editor, Guidebook to the geology of the Wasatch and Uinta Mountains transition area: Intermountain Association of Petroleum Geologists, Tenth Annual Field Conference, p. 46–53.

Hiscock, A.I., Kleber, E.J., Hylland M.D., and McDonald, G.N., 2023, Digging up evidence of past earthquakes in Salt Lake Valley: Utah Geological Survey, Survey Notes, v. 55, no. 2, p. 3–5, https://doi.org/10.34191/SNT-55-2.

Hunt, C.B., editor, 1982, Pleistocene Lake Bonneville, ancestral Great Salt Lake, as described in the notebooks of G.K. Gilbert, 1875–1880: Brigham Young University Geology Studies. v. 29, pt. 1, 225 p.

Hylland, M.D., DuRoss, C.B., McDonald, G.N., Olig, S.S., Oviatt, C.G., Mahan, S.A., Crone, A.J., and Personius, S.F., 2012, Basin-floor Lake Bonneville stratigraphic section as revealed in paleoseismic trenches at the Baileys Lake site, West Valley fault zone, Utah, *in* Hylland, M.D., and Harty, K.M., editors, Selected topics in engineering and environmental geology in Utah: Utah Geological Association Publication 41, p. 175–193.

Hylland, M.D., DuRoss, C.B., McDonald, G.N., Olig, S.S., Oviatt, C.G., Mahan, S.A., Crone, A.J., and Personius, S.F., 2014, Late Quaternary paleoseismology of the West Valley fault zone—insights from the Baileys Lake trench site, *in* DuRoss, C.B., and Hylland, M.D., Evaluating surface faulting chronologies of graben-bounding faults in Salt Lake Valley, Utah—new paleoseismic data from the Salt Lake City segment of the Wasatch fault zone and the West Valley fault zone—Paleoseismology of Utah, Volume 24: Utah Geological Survey Special Study 149, p. 41–76, 8 appendices, 1 plate, https://doi.org/10.34191/SS-149.

Hylland, M.D., Hiscock, A.I., McDonald, G.N., DuRoss, C.B., Mahan, S.A., Briggs, R.W., Personius, S.F., and Reitman, N.G., 2022, Paleoseismic investigation of the Taylorsville fault at the Airport East Site, West Valley fault zone, Salt Lake County, Utah—Paleoseismology of Utah, Volume 29: Utah Geological Survey Special Study 169, 29 p., 7 appendices, 2 plates, https://doi.org/10.34191/SS-169.

Kaliser, B.N., 1976, Earthquake fault map of a portion of Salt Lake County, Utah: Utah Geological and Mineral Survey Map 42, https://doi.org/10.34191/M-42.

Keaton, J.R., 1987, Potential consequences of earthquake induced regional tectonic deformation along the Wasatch Front, north-central Utah, *in* McCalpin, J., editor, Proceedings of the 23rd Symposium on Engineering Geology and Soils Engineering: Boise, Idaho Department of Transportation, p. 19–34

Keaton, J.R., and Currey, D.R., 1989, Earthquake hazard evaluation of the West Valley fault zone in the Salt Lake City urban area, Utah: Salt Lake City, Dames & Moore, unpublished technical report prepared for U.S. Geological Survey, contract no. 14-08-0001-G1397, 69 p. (Subsequently published in 1993 as Utah Geological Survey Contract Report 93-7, https://doi.org/10.34191/CR-93-7.)

Keaton, J.R., Currey, D.R., and Olig, S.J., 1987, Paleoseismicity and earthquake hazards evaluation of the West Valley fault zone, Salt Lake City urban area, Utah: Salt Lake City, Dames & Moore and University of Utah Department of Geography, unpublished technical report prepared for U.S. Geological Survey, contract no. 14-08-0001-22048, 55 p., + 33 p. appendix. (Subsequently published in 1993 as Utah Geological Survey Contract Report 93-8, https://doi.org/10.34191/CR-93-8.)

Kleber, E.J., McKean, A.P., Hiscock, A.I., Hylland, M.D., Hardwick, C.L., McDonald, G.N., Anderson, Z.W., Bowman, S.D., Willis, G.C., and Erickson, B.A., 2021, Geologic setting, ground effects, and proposed structural model for the 18 March 2020 M_w 5.7 Magna, Utah, Earthquake: Seismological Research Letters, v. 92, no. 2A, p. 710–724, https://doi.org/10.1785/0220200331.

Kleinfelder, Inc., 1999, Geologic investigation, Salt Palace expansion, phase II, NW corner 200 South and West Temple, Salt Lake City, Utah: unpublished consultant report prepared for Salt Lake County c/o Construction Control Corporation, variously paginated.

Le Bas, M.J., LeMaitre, R.W., Streckeisen, A., and Zanettin, B., 1986, A chemical classification of volcanic rocks based on the total alkali-silica diagram: Journal of Petrology, v. 27, p. 745–750.

Leeflang, B.T., 2008, Ground displacement investigations in downtown Salt Lake City, Utah, using the cone penetrometer: Salt Lake City, University of Utah, M.S. thesis, 161 p.

Leeflang, W.E., and Everitt, B.L., 1993, Fault trench investigation and report—CH Dredge Company metal building: unpublished consultant report prepared for Richard Daems and Associates, 7 p.

Liberty, L., 2016, Seismic profiling in downtown Salt Lake City—mapping the Wasatch fault with seismic velocity and reflection methods from a land streamer: unpublished contract deliverable report prepared for U.S. Geological Survey, award number G12AP20078, 26 p.

Liberty, L., 2018, Seismic profiling in downtown Salt Lake City—mapping the Wasatch fault with seismic velocity and reflection methods from a land streamer: unpublished contract deliverable report prepared for U.S. Geological Survey, award number G17AP00052, 49 p.

Liberty, L.M., St. Clair, J., and McKean, A.P., 2021, A broad, distributed active fault zone lies beneath Salt Lake City, Utah: The Seismic Record, v. 1, no. 1, p. 35–45, https://doi.org/10.1785/0320210009.

Lowe, M., Kirby, S.M., and Harty, K.M., 2018, Geologic map of the Farmington quadrangle, Salt Lake and Davis Counties, Utah: Utah Geological Survey Map 279DM, 2 plates, scale 1:24,000, https://doi.org/10.34191/M-279DM.

Lund, W.R., 2005, Consensus preferred recurrence interval and vertical slip rate estimates—review of Utah paleoseismic-trenching data by the Utah Quaternary Fault Parameters Working Group: Utah Geological Survey Bulletin 134, 109 p., 5 appendices, https://doi.org/10.34191/B-134.

Machette, M.N., Personius, S.F., and Nelson, A.R., 1992, Paleoseismology of the Wasatch fault zone—a summary of recent investigations, interpretations, and conclusions, *in* Gori, P.L., and Hays, W.W., editors, Assessment of regional earthquake hazards and risk along the Wasatch Front, Utah: U.S. Geological Survey Professional Paper 1500–A, p. A1–A59.

Mann, C.D., 1974, Clastic Laramide sediments of the Wasatch hinterland, northeastern Utah: Salt Lake City, University of Utah, M.S. thesis, 112 p.

Marine, I.W., and Price, D., 1964, Geology and ground-water resources of the Jordan Valley, Utah: Utah Geological and Mineralogical Survey, Water-Resources Bulletin 7, 67 p., https://doi.org/10.34191/WRB-7.

Marsell, R.E., and Threet, R.L., 1960, Geologic map of Salt Lake County, Utah, *in* Crawford, A.L., editor, 1964, Geology of Salt Lake County: Utah Geological and Mineralogical Survey Bulletin 69, 190 p., 1 plate, scale 1:63,360, https://doi.org/10.34191/B-69.

McDonald, G.N., Kleber, E.J., Hiscock, A.I., Bennett, S.E.K., and Bowman, S.D., 2020, Fault trace mapping and surface-fault-rupture special study zone delineation of the Wasatch fault zone, Utah and Idaho: Utah Geological Survey Report of Investigation 280, 23 p., https://doi.org/10.34191/RI-280.

McGee, D., Quade, J., Edwards, R.L., Broecker, W.S., Cheng, H., Reiners, P.W., and Evenson, P., 2012, Lacustrine cave carbonates—novel archives of paleohydrologic change in the Bonneville Basin (Utah, USA): Earth and Planetary Science Letters, v. 351–352, p. 182–194.

McKean, A.P., 2017, Whole-rock geochemical data for the Salt Lake City North, Sugar House, and Draper quadrangles, Utah: Utah Geological Survey Open-File Report 663, 5 p., https://doi.org/10.34191/OFR-663.

McKean, A.P., 2019a, Geologic map of the Saltair NE quadrangle, Salt Lake and Davis Counties, Utah: Utah Geological Survey Map 282DM, 28 p., 2 plates, scale 1:24,000, https://doi.org/10.34191/M-282DM.

McKean, A.P., 2019b, Geologic map of the Salt Lake City South quadrangle, Salt Lake County, Utah: Utah Geological Survey Map 283DM, 13 p., 2 plates, scale 1:24,000, https://doi.org/10.34191/M-283DM.

McKean, A.P., 2020, Geologic map of the Sugar House quadrangle, Salt Lake County, Utah: Utah Geological Survey Map 285DM, 27 p., 2 plates, scale 1:24,000, https://doi.org/10.34191/M-285DM.

McKean, A.P., Apatite to Zircon, Inc., and O'Sullivan, P., 2016, U-Pb detrital zircon geochronology results for the Salt Lake City North quadrangle, Utah: Utah Geological Survey Open-File Report 657, variously paginated, https://doi.org/10.34191/OFR-657.

McKean, A.P., Beukelman, G.S., Erickson, B.A., Hiscock, A.I, 2012, Monitoring a slow-moving urban landslide, Springhill Landslide, North Salt Lake, Davis County, Utah: AEG News, v. 55— Annual Meeting Program with Abstracts, p. 69.

McKean, A.P., and Hylland, M.D., 2019a, Geologic map of the Baileys Lake quadrangle, Salt Lake and Davis Counties, Utah: Utah Geological Survey Map 281DM, 28 p., 2 plates, scale 1:24,000, https://doi.org/10.34191/M-281DM.

McKean, A.P., and Hylland, M.D., 2019b, Post-Lake Bonneville migration of the Jordan River, Salt Lake Valley, Utah [abstract and poster], *in* Lund, W.R., McKean, A.P., and Bowman, S.D., editors, Proceedings volume—2018 Lake Bonneville geologic conference and short course, October 3–6, 2018: Utah Geological Survey Miscellaneous Publication 170, variously paginated, https://doi.org/10.34191/MP-170.

McKean, A.P., and Nevada Isotope Geochronology Laboratory [NIGL], 2016, $^{40}Ar/^{39}Ar$ geochronology results for the Salt Lake City North quadrangle, Utah: Utah Geological Survey Open-File Report 658, 6 p., https://doi.org/10.34191/OFR-658.

Miller, D.M., 2016, The Provo shoreline of Lake Bonneville, *in* Oviatt, C.G., and Shroder, J.F., Jr., editors, Lake Bonneville—a scientific update: Amsterdam, Netherlands, Elsevier, Developments in earth surface processes, v. 20, chapter 7, p. 127–144.

Miller, D.M., Oviatt, C.G., Dudash, S.L., and McGeehin, J.P., 2005, Late Holocene highstands of Great Salt Lake at Locomotive Springs, Utah [abs.]: Geological Society of America Abstracts with Programs, v. 37, no. 7, p. 335.

Miller, R.D., 1980, Surficial geologic map along part of the Wasatch Front, Salt Lake Valley, Utah: U.S. Geological Survey Miscellaneous Field Studies Map MF-1198, 13 p., scale 1:100,000.

Morris, H.T., and Lovering, T.S., 1961, Stratigraphy of the East Tintic Mountains, Utah: U.S. Geological Survey Professional Paper 361, 145 p.

Murchison, S.B., 1989, Fluctuation history of Great Salt Lake, Utah, during the last 13,000 years: Salt Lake City, University of Utah, Ph.D. dissertation, 137 p.

Nelson, S.T., Harris, R.A., Dorais, M.J., Heizler, M., Constenius, K.N., and Barnett, D.E., 2002, Basement complexes of the Wasatch fault, Utah, provide new limits on crustal accretion: Geology, v. 30, p. 831–834, data repository item 2002097.

Oaks, R.J., Jr., Smith, K.A., Janecke, S.U., Perkins, M.E., and Nash, W.P., 1999, Stratigraphy and tectonics of Tertiary strata of southern Cache Valley, north-central Utah, *in* Spangler, L.E., and Allen, C.J., editors, Geology of Northern Utah and Vicinity: Utah Geological Association 27, p. 71–110.

Osmond. J.C., Hewitt, W.P., and Van Horn, R., 1965, Engineering implications and geology, Hall of Justice excavation, Salt Lake City, Utah: Utah Geological and Mineralogical Survey Special Study 11, 36 p., https://doi.org/10.34191/SS-11.

Oviatt, C.G., 1986, Geologic map of the Honeyville quadrangle, Box Elder and Cache Counties, Utah: Utah Geological and Mineral Survey Map 88, 13 p., 2 plates, scale 1:24,000, https://doi.org/10.34191/M-88.

Oviatt, C.G., 2014, The Gilbert episode in the Great Salt Lake basin, Utah: Utah Geological Survey Miscellaneous Publication 14-3, 20 p., https://doi.org/10.34191/MP-14-3.

Oviatt, C.G., 2015, Chronology of Lake Bonneville, 30,000 to 10,000 yr B.P.: Quaternary Science Reviews, v. 110, p. 166–171, Appendix A supplementary data available online, http://dx.doi.org/10.1016/j.quascirev.2014.12.016.

Oviatt, C.G., Currey, D.R., and Miller, D.M., 1990, Age and paleoclimatic significance of the Stansbury shoreline of Lake Bonneville, northeastern Great Basin: Quaternary Research, v. 33, p. 291–305.

Oviatt, C.G., Miller, D.M., McGeehin, J.P., Zachary, C., and Mahan, S., 2005, The Younger Dryas phase of Great Salt Lake, Utah, USA: Palaeogeography, Palaeoclimatology, Palaeoecology, v. 219, no. 3–4, p. 263–284.

Pang, G., Koper, K.D., Mesimeri, M., Pankow, K.L., Baker, B., Farrell, J., Holt, J., Hale, J.M., Roberson, P., Burlacu, R., Pechmann, J.C., Whidden, K., Holt, M.M., Allam, A., DuRoss, C., 2020, Seismic analysis of the 2020 Magna, Utah, earthquake sequence–evidence for a listric Wasatch fault: Geophysical Research Letters, v. 47, issue 18, 10 p., https://doi.org/10.1029/2020GL089798

Parry, W.T., and Bruhn, R.L., 1986, Pore fluid and seismogenic characteristics of fault rock at depth on the Wasatch fault, Utah: Journal of Geophysical Research, v. 91, no. B1, p. 730–744.

Personius, S.F., and Scott, W.E., 1992, Surficial geologic map of the Salt Lake City segment and parts of the adjacent segments of the Wasatch fault zone, Davis, Salt Lake, and Utah Counties, Utah: U.S. Geological Survey Miscellaneous Investigations Series Map I-2106, 1 plate, scale 1:50,000.

Radkins, H., Murphy, M., and Schuster, G.T., 1989, Subsurface map and seismic risk analysis of the Salt Lake Valley: Utah Geological and Mineral Survey Open-File Report 152, 82 p., https://doi.org/10.34191/OFR-152.

Reimer, P., Austin, W., Bard, E., Bayliss, A., Blackwell, P., Bronk Ramsey, C., Butzin, M., Cheng, H., Edwards, R., Friedrich, M., Grootes, P., Guilderson, T., Hajdas, I., Heaton, T., Hogg, A., Hughen, K., Kromer, B., Manning, S., Muscheler, R., Palmer, J., Pearson, C., van der Plicht, J., Reimer, R., Richards, D., Scott, E., Southon, J., Turney, C., Wacker, L., Adolphi, F., Büntgen, U., Capano, M., Fahrni, S., Fogtmann-Schulz, A., Friedrich, R., Köhler, P., Kudsk, S., Miyake, F., Olsen, J., Reinig, F., Sakamoto, M., Sookdeo, A., and Talamo, S., 2020, The IntCal20 Northern Hemisphere radiocarbon age calibration curve (0–55 cal kBP): Radiocarbon, v. 62., no. 4, p. 725–75, doi:10.1017/RDC.2020.41.

Rigby, J.K., 1959, Upper Devonian unconformity in central [northern] Utah: Geological Society of America Bulletin, v. 70, p. 207–218.

Rigby, J.K., and Clark, D.L., 1962, Devonian and Mississippian systems in central Utah: Brigham Young University Geology Studies, v. 9, pt. 1, p. 17–25.

Rigo, R.J., 1968, Middle and Upper Cambrian stratigraphy in the autochthon and allochthon of northern Utah: Brigham Young University Geology Studies, v. 15, part 1, p. 31–66.

Robison, R.M., Burr, T.N., Murchison, S.B., Keaton, J.R., and Currey, D.R., 1991, Investigating fault rupture hazards — An example from the Wasatch fault zone, Utah, *in* Cassaro, M.A., editor, Lifeline earthquake engineering: Technical Council on Lifeline Engineering Monograph No. 4, American Society of Civil Engineers, Proceedings of the Third Conference, p. 601–610.

Sandberg, C.A., and Gutschick, R.C., 1979, Guide to conodont biostratigraphy of Upper Devonian and Mississippian rocks along the Wasatch Front and Cordilleran hingeline, Utah; Brigham Young University Geology Studies, v. 26, pt. 3, p. 107–133.

Scott, W.E., and Shroba, R.R., 1985, Surficial geologic map of an area along the Wasatch fault zone in Salt Lake Valley, Utah: U.S. Geological Survey Open-File Report 85-448, 18 p., 2 plates, scale 1:24,000.

Sergent, Hauskins & Beckwith, 1991, Report, fault investigation, Washington Elementary School, 158 Quince Avenue, Salt Lake City, Utah: unpublished consultant report prepared for Salt Lake City School District, 34 p.

Silberling, N.J., and Nichols, K.M., 1992, Depositional cycles of the Upper Devonian-Lower Mississippian Limestone succession in the southern Lakeside Mountains, Utah, with an appendix on the identification and age interpretations of conodont faunas by R.G. Stamm, *in* Wilson, J.R., editor, Field guide to geologic excursions in Utah and adjacent areas of Nevada, Idaho, and Wyoming, prepared for the Geological Society of America Rocky Mountain Section meeting in Ogden, Utah, May 13–15, 1992: Utah Geological Survey Miscellaneous Publication 92-3, p. 131–145, https://doi.org/10.34191/MP-92-3.

Simon Bymaster, Inc., 1999, Report of geological investigation Salt Palace Convention Center expansion project, 100 South West Temple Street, Salt Lake City, Utah: unpublished consultant report prepared for Salt Lake County c/o Construction Control Corporation, variously paginated.

Smidinger, B., 2017, Sixth five-year review report for Rose Park Sludge Pit Superfund Site Salt Lake County, Utah: Utah Department of Environmental Quality Division of Environmental Response and Remediation report prepared for U.S. Environmental Protection Agency Region 8 Denver, Colorado, dated 9/14/17, variously paginated, online, https://semspub.epa.gov/work/08/100001613.pdf, accessed July 30, 2019.

Solomon, B.J., 1998, New evidence for the age of faulting on the West Valley fault zone: Utah Geological Survey, Survey Notes, v. 30, no. 3, p. 8 and 13, https://doi.org/10.34191/SNT-30-3.

Solomon, B.J., Biek, R.F., and Smith, T.W., 2007, Geologic map of the Magna quadrangle, Salt Lake County, Utah: Utah Geological Survey Map 216, 2 plates, scale 1:24,000, https://doi.org/10.34191/M-216 (Subsequently published in 2018 as Utah Geological Survey Digital Reproduction M-216DM, https://doi.org/10.34191/M-216DM).

Taylor, M.E., Landing, E., and Gillett, S.L., 1981, The Cambrian-Ordovician transition in the Bear River Range, Utah-Idaho—a preliminary evaluation, *in* Taylor, M.E., editor, Short papers for the second international symposium on the Cambrian System: U.S. Geological Survey Open-File Report 81-743, p. 222–227.

Tooker, E.W., 1999, Geology of the Oquirrh Mountains, Utah: U.S. Geological Survey Open-File Report 99-571, 150 p., scale 1:50,000.

Trexler, J.H., Jr., 1992, The Devonian-Mississippian Stansbury Formation at Stansbury Island and in the northeastern Stansbury Mountains, Utah, *in* Wilson, J.R., editor, Field guide to geologic excursions in Utah and adjacent areas of Nevada, Idaho, and Wyoming: Utah Geological Survey Miscellaneous Publication 92-3, p. 161–169, https://doi.org/10.34191/MP-92-3.

USDA Agricultural Adjustment Administration, 1937, Aerial photography, Project AAL frames 1–28 to 54, 1–108 to110, and 2–1 to 22 dated 9–19–1937, black and white, approximate scale 1:20,000.

USDA Agricultural Adjustment Administration, 1946, Aerial photography, Project AAL frames 1B–161 to 162 and 1B–179–181 dated 8–16–1946, black and white, scale 1:20,000.

USDA Agricultural Commodity Stabilization Service, 1958, Aerial photography, Project AAL frames 6V–15 to 33, 6V–104 to 108, 11V–2 to 15, 11V–36 to 53, 11V–134 to 167, 12V–44 to 54, 12V–68 to 73, 12V–158 to 165 dated 5–27–1958, frames 32V–90 to 94 dated 9–6–1958, and frames 35V–29 to 48 dated 10–15–1958, black and white, scale 1:10,000.

USDA Agricultural Stabilization and Conservation Service, 1971, Aerial photography, Project AAL, frames 2MM–4 to 16 dated 10–9–1971, black and white, approximate scale 1:20,000.

USDA Forest Service, 1963, Aerial photography, Project ELK frames 2–4 to 8 dated from 6–25–1963, black and white, scale 1:15,840.

USDA National Agriculture Imagery Program (NAIP), 2009, Digital aerial stereo-photography, resolution 12 microns or 2117 pixels per inch, 3-band natural color, scale 1:40,000.

U.S. Environmental Protection Agency (EPA), 1992, Superfund record of decision—Portland Cement (kiln dust #2 & #3), UT: U.S. Environmental Protection Agency Region VIII, Office of Emergency and Remedial Response, report number EPA/ROD/R08-92/056, variously paginated, available online https://www.epa.gov/nscep, accessed April 27, 2017.

U.S. Environmental Protection Agency (EPA), undated, Superfund site—Portland Cement (kiln dust 2 & 3) Salt Lake City, UT—site details: Online, https://cumulis.epa.gov/supercpad/CurSites/csitinfo.cfm?id=0800690&msspp=med, accessed June 28, 2017.

U.S. Geological Survey, 1934, Salt Lake City and vicinity, Utah: Topographic map, 1:24,000 scale.

U.S. Natural Resources Conservation Service (NRCS), 2010, Web soil survey (WSS) database for Salt Lake area, Utah: Online, https://websoilsurvey.nrcs.usda.gov/app/WebSoilSurvey.aspx, accessed January 30, 2013.

Utah Geospatial Resource Center (UGRC), State Geographic Information Database, 1977, 1 meter black and white Salt Lake County digital orthophoto quads: Online, https://gis.utah.gov/data/aerial-photography/doq/, accessed May 2013.

Utah Geospatial Resource Center (UGRC), State Geographic Information Database, mid-1990s, 1 meter black and white digital orthophoto quads: Online, https://gis.utah.gov/data/aerial-photography/doq/, accessed January 2013.

Utah Geospatial Resource Center (UGRC), State Geographic Information Database, 2006, 2 meter lidar elevation data: Online, https://gis.utah.gov/data/aerial-photography/naip/, September 2013.

Utah Geospatial Resource Center (UGRC), State Geographic Information Database, 2011a, National Agricultural Imagery Program 1 meter orthophotography: Online, https://gis.utah.gov/data/aerial-photography/naip/, accessed June 2012.

Utah Geospatial Resource Center (UGRC), State Geographic Information Database, 2019, Hexagon licensed imagery 15 cm aerial photography: Online, https://gis.utah.gov/data/aerial-photography/, accessed December 2021.

Utah Geospatial Resource Center (UGRC), State Geographic Information Database, 2011b, 1 meter lidar elevation data: Online, http://gis.utah.gov/data/elevation-terrain-data/2011-lidar/, accessed June 2012.

Utah Geospatial Resource Center (UGRC), State Geographic Information Database, 2013–2014, 0.5-meter Wasatch Front LiDAR elevation data: Online, Utah http://gis.utah.gov/data/elevation-terrain-data/2013-2014-lidar/.

Utah Geological Survey (UGS), 2012, Update on Springhill landslide: Online, https://geology.utah.gov/hazards/landslides/springhill-landslide-north-salt-lake/update-on-springhill-landslide/, dated 7/12/2012, accessed August 2019.

Utah Geological Survey (UGS), undated, Parkway Drive landslide, North Salt Lake: Online, https://geology.utah.gov/hazards/landslides/parkway_drive_landslide/, accessed August 2019.

Van Horn, R., 1979, Surficial geologic map of the Salt Lake City South quadrangle, Salt Lake County, Utah: U.S. Geological Survey Miscellaneous Investigations Series Map I-1173, 1 plate, scale 1:24,000.

Van Horn, R., 1981, Geologic map of pre-Quaternary rocks of the Salt Lake City North quadrangle, Davis and Salt Lake Counties, Utah: U.S. Geological Survey Miscellaneous Investigations Series Map I-1330, 1 plate, scale 1:24,000.

Van Horn, R., 1982, Surficial geologic map of the Salt Lake City North quadrangle, Davis and Salt Lake Counties, Utah: U.S. Geological Survey Miscellaneous Investigations Series Map I-1404, 1 plate, scale 1:24,000.

Van Horn, R., and Crittenden, M.D., Jr.,1987, Map showing surficial units and bedrock geology of the Fort Douglas quadrangle and parts of the Mountain Dell and Salt Lake City North quadrangles, Davis, Salt Lake, and Morgan Counties, Utah: U.S. Geological Survey Miscellaneous Investigations Series Map I-1762, 1 plate, scale 1:24,000.

Willis, G.C., and Jensen, M.E., 2000, Tertiary rocks of Antelope Island, Davis County, northern Utah, *in* King, J.K., and Willis, G.C., editors, The geology of Antelope Island, Davis County, Utah: Utah Geological Survey Miscellaneous Publication 00-1, p. 49–70, https://doi.org/10.34191/MP-00-1.

Willis, G.C., Yonkee, W.A., Doelling, H.H., and Jensen, M.E., 2010, Geology of Antelope Island State Park, Utah, in Sprinkel, D.A., Chidsey, T.C., Jr., and Anderson, P.B., editors, Geology of Utah's parks and monuments, third edition: Utah Geological Association Publication 28, p. 349–377.

Whitmeyer, S.J., and Karlstrom, K.E., 2007, Tectonic model for the Proterozoic growth of North America: Geosphere, v. 3, no. 4, p. 220–259.

Yonkee, W.A., and Barnett, D.A., 2000, Geologic and hydrogeologic setting of the upper Emigration Canyon area: unpublished consultant's report, 65 p.

Yonkee, W.A., DeCelles, P.G., and Coogan, J., 1997, Kinematics and synorogenic sedimentation of the eastern frontal part of the Sevier orogenic wedge, northern Utah: Brigham Young University Geology Studies, v. 42, part 1, p. 355–380.

Yonkee, W.A., and Weil, A.B., 2011, Evolution of the Wyoming salient of the Sevier fold-thrust belt, northern Utah to western Wyoming, *in* Sprinkel, D.A., Yonkee, W.A., and Chidsey, T.C., Jr., editors, Sevier thrust belt— northern and central Utah and adjacent areas: Utah Geological Association Publication 40, p. 1–56.

Yonkee, W.A., and Weil, A.B., 2015, Tectonic evolution of the Sevier and Laramide belts within the North American Cordilleran orogenic system: Earth Science Reviews, v. 150, p. 531–593, https://doi.org/10.1016/j.earscirev.2015.08.001.

Yonkee, W.A., Willis, G.C., and Doelling, H.H., 2000, Petrology and geologic history of the Precambrian Farmington Canyon Complex, Antelope Island, Utah, *in* King, J.K., and Willis, G.C., editors, The geology of Antelope Island, Davis County, Utah: Utah Geological Survey Miscellaneous Publication 00–1, p. 5–36, https://doi.org/10.34191/MP-00-1.

Zoback, M.L., 1983, Structure and Cenozoic tectonism along the Wasatch fault zone, Utah, *in* Miller, D.M., Todd, V.R., and Howard, K.A., editors, Tectonic and stratigraphic studies in the eastern Great Basin: Geological Society of America Memoir 157, p. 3–27.

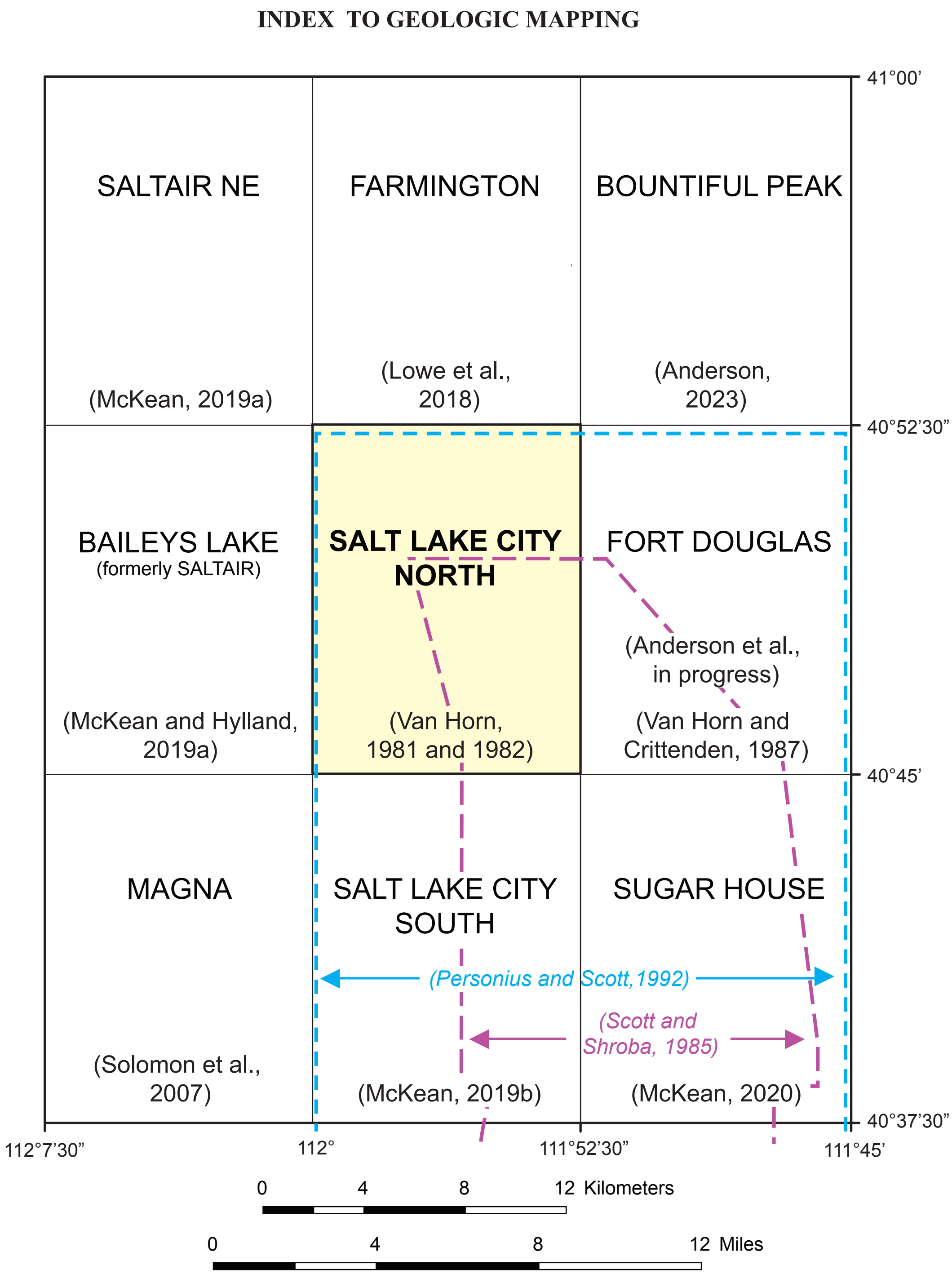

Figure 1. Index map showing selected geologic maps available for the Salt Lake City North quadrangle and surrounding 7.5′ quadrangles.

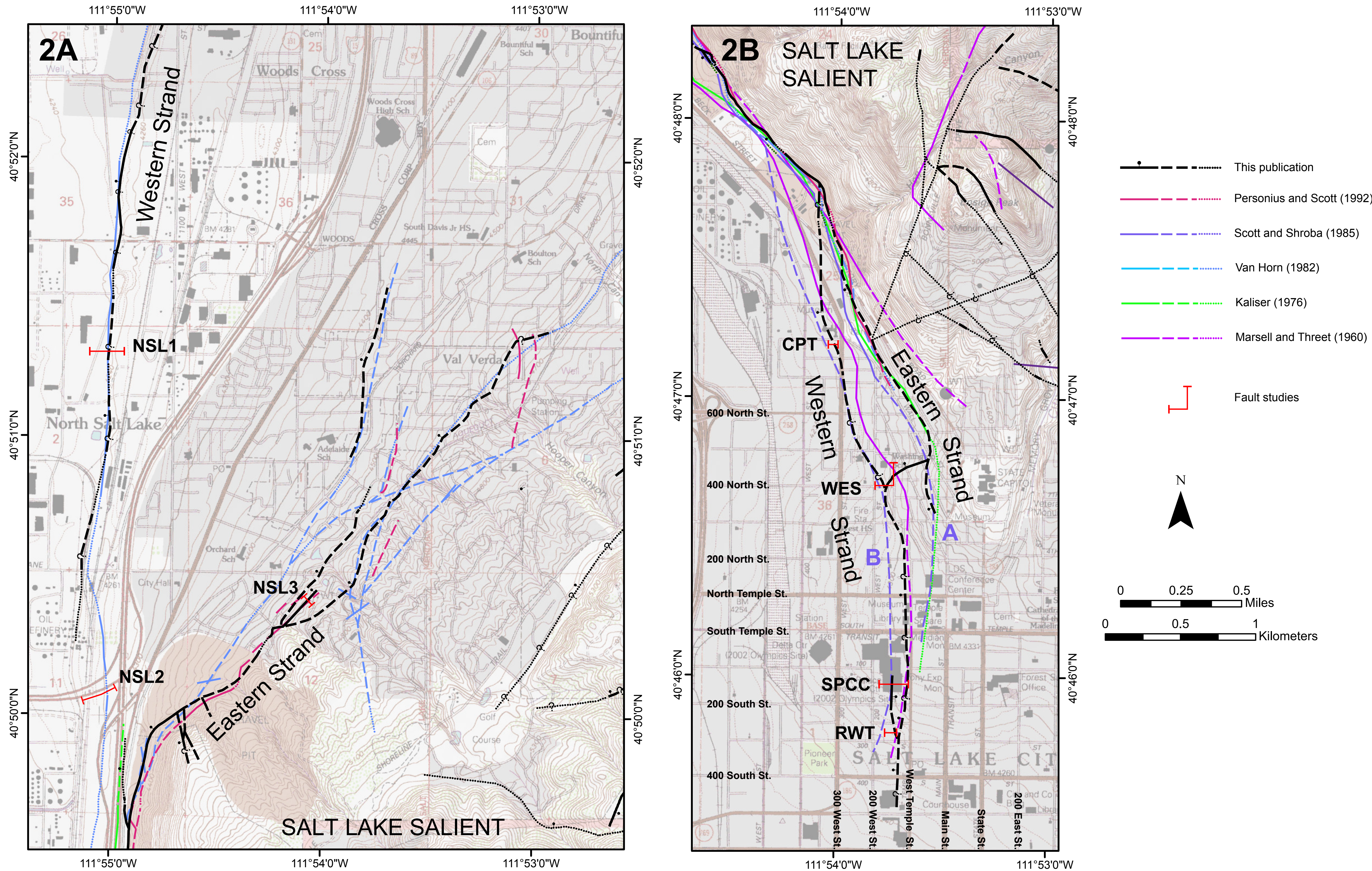

Figure 2. *Map showing various interpretations of the extent of the northern (2A) and southern (2B) part of the Warm Springs fault from previous fault mapping (Marsell and Threet, 1960; Kaliser, 1976; Van Horn, 1981, 1982; Scott and Shroba, 1985; Personius and Scott, 1992; this report). For the northern part of the fault zone is separated into an eastern and western strand (2A), on the western strand Robison et al. (1991) boring and trench locations are shown by locations NSL1 and NSL2. Approximate trench location on the eastern strand from Applied Geotechnical Engineering Consultants, Inc. (1994) is at NSL3. For the southern part of the fault zone (2B) green faults labeled "A" and "B" are from Scott and Shroba (1985) and are similar to our eastern and western strands. Fault study locations are marked on the figure by CPT for the cone penetrometer test study between 800 North and Reed Avenue, WES for Washington Elementary School site, and SPCC for the Salt Palace Convention Center expansion project. See the Surface-Fault Rupture section for more information. Base map is the 1998 USGS topographic map.*

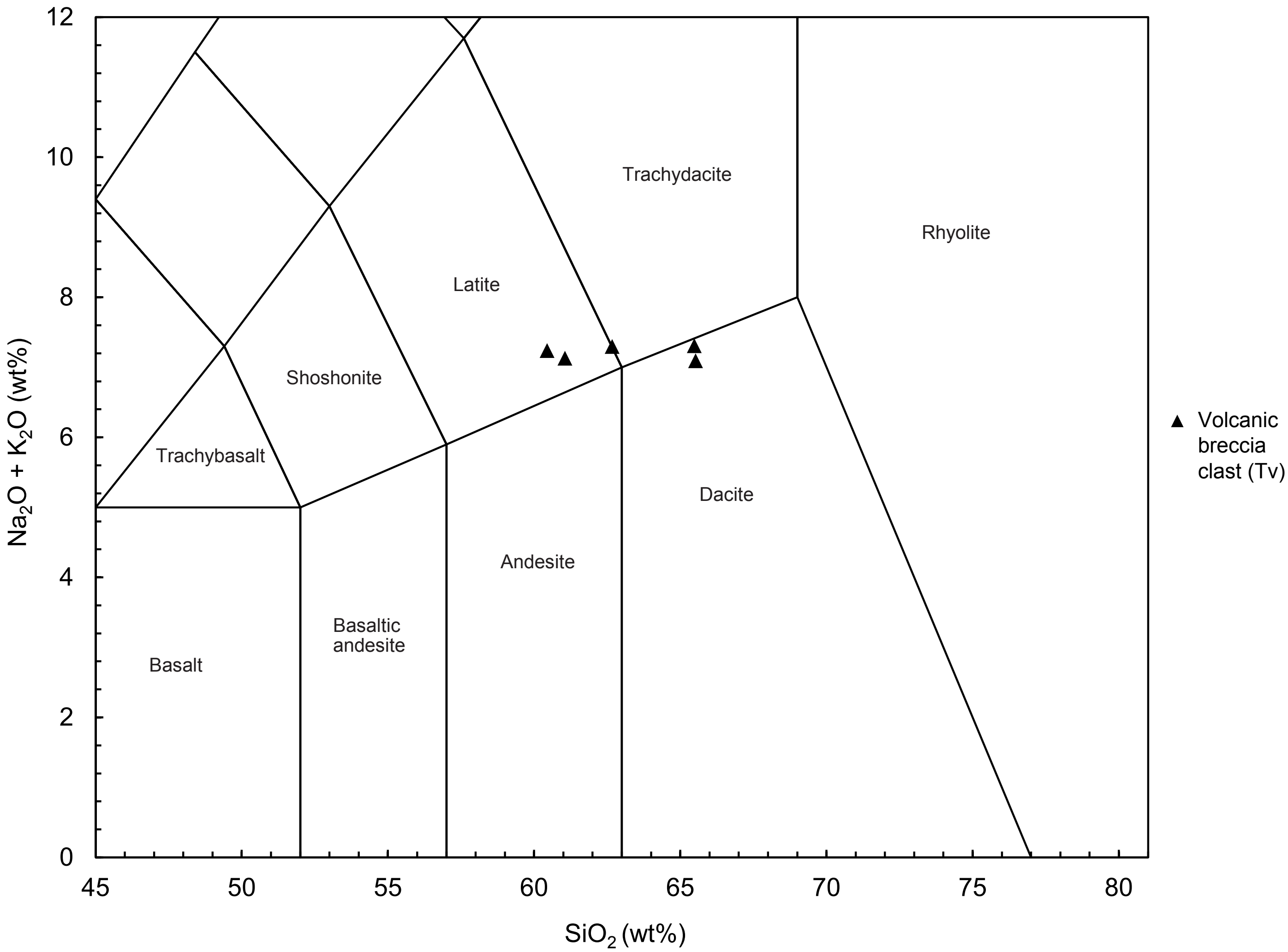

***Figure 3.** Total alkali-silica classification for Paleogene volcaniclastic conglomerate clasts (unit Tv) from the Salt Lake City North quadrangle (values have been normalized to 100% on a volatile-free basis); see McKean (2017) for whole-rock geochemical data (classification diagram from Le Bas et al., 1986.*

Table 1. *Age of major shoreline occupations of Lake Bonneville, Gilbert-episode lake, and Great Salt Lake and shoreline elevations in the Salt Lake City North quadrangle.*

Lake Cycle and Phase	Shoreline (map symbol)	Age		Elevation feet (meters)
		radiocarbon years (^{14}C yr B.P.)	calibrated years (cal yr B.P.)[1]	
Lake Bonneville				
Transgressive phase	Stansbury (S) shorelines	22,000–20,000[2]	26,000–24,000	4470–4500 (1362–1372)
	Transgressive shorelines (t)	20,000–15,200[3]	24,000–18,500	5100–5180 (1554–1579)
	Bonneville (B) flood	~15,200–15,000[4]	~18,500–18,000	5180–5200 (1579–1585)
Overflowing phase	Provo (P)	15,000–12,600[5]	18,000–15,000	4820–4860 (1469–1482)
Regressive phase	Regressive shorelines (r)	12,600–11,500[5]	15,000–13,000	~4600–4700+ (~1402–1433+)
Gilbert-episode lake	Gilbert (G)	10,000[6]	11,500	4245–4250 (1294–1295)
Great Salt Lake				
	early Holocene highstand	9700–9400[7]	11,000–10,500	4225–4230? (1288–1289)
	late Holocene highstand (H)	4200–2100[8]	5000–2000	4217–4221 (1285–1287)
	Historical highstand (h)		late 1860s to early 1870s and 1986–87[9]	4212 (1284)

1 All calibrations made using OxCal ^{14}C calibration and analysis software (version 4.4; Bronk Ramsey, 2009; using the IntCal20 calibration curve of Reimer et al., 2020), rounded to the nearest 500 years. B.P. = before present, meaning the number of years before A.D. 1950

2 Oviatt et al. (1990)

3 Oldest and youngest age from the youngest Stansbury shoreline and oldest Bonneville shoreline, respectively (see references 2 and 4)

4 Oviatt (2015), Miller (2016), and references therein

5 Godsey et al. (2005, 2011), Oviatt (2015), Miller (2016) for the timing of the occupation of the Provo shoreline and subsequent regression of Lake Bonneville to near Great Salt Lake level. Alternatively, data in Godsey et al. (2005) suggest that regression began shortly after 16.5 cal ka (for example sample Beta-153158, with an age of 13,660 ± 50 ^{14}C yr B.P. [16.5 cal ka] from 1.5 m below the Provo shoreline). Also, lacustrine carbonate deposits in caves reported by McGee et al. (2012) seem to support an earlier Lake Bonneville regression beginning around 16.4 cal ka.

6 Gilbert-episode highstand may have been very short lived; age represents lake culmination (Oviatt et al., 2005; Oviatt, 2014)

7 Murchison (1989), Currey and James (1982)

8 Miller et al. (2005)

9 Arnow and Stephens (1990)

Table 2. *Summary of oil and gas exploration drill holes/wells from the Salt Lake City North 7.5' quadrangle.*

.

API Number	Well Name	Latitude (°N)	Longitude (°W)	Total Depth ft (m)	Year Completed	Lithology Notes
4303516543	Western Petroleum Drilling Co. #1	40.80393	111.95605	1985 (604)	1931	Pleistocene mollusks at 884 ft (Berry and Crawford [1932] in Arnow and Mattick [1968]); Tertiary marl, volcanic ash and tuff, including a 2.5-ft bed of tuff, at 1308 ft (Eardley and Hass [1936] in Cook and Berg [1961]); Tertiary at TD (Hansen and Scoville [1955] in Cook and Berg [1961])
4303530001	Gillmor Fee 1	40.81483	111.95596	6120 (1865)	1974	High gamma ray from 3600 to 4500 ft, interpreted by authors to be Tertiary volcanic rocks interval, followed by Mesozoic and/or Paleozoic strata at 4500 to TD
4303530004	Gillmor Fee 1-A-X	40.81805	111.95500	3756 (1145)	1976	Tertiary at TD

Source:

Utah Division of Oil, Gas and Mining; https://oilgas.ogm.utah.gov/oilgasweb/live-data-search/lds-logs/logs-lu.xhtml, acessed June 12, 2014

Location data in NAD83